Analyses of Lunar Transient Phenomena (LTP) Observations from 557–1994 A.D.

Winifred S. Cameron
200 Rojo Drive, Sedona, Arizona 86351

Pages: 82
Plates: 2
Tables: 10
Figures: 5

Proposed Running Head: Analysis of LTP vs. Hypotheses

Editorial correspondence to:

Mrs. Winifred S. Cameron

200 Rojo Drive

Sedona, AZ 86351-9329

Phone: (928) 284-9657

E-mail: stuartjl@ieee.org

ABSTRACT

Literature and received reports of lunar transient phenomena (LTP) in lunar programs of observations provided a collection of 2254 total of observations, from 557-1994 A.D. with sufficient information for auxiliary data analysis. Among the 2254 there were 645 that were independently confirmed and/or permanently recorded in photographs, spectra, photometry, and polarimetry. These are designated by **+.** In study of these reports 448 were found that could not be explained by terrestrial atmospheric or instrumental effects, so are probably intrinsically lunar and are designated * and + for those confirmed or permanently recorded ***+**.

Observations fell into five categories (Bright, Dark, Red, Blue and Gaseous). It was also found that about a dozen features provided >60% of all observations. Separate analyses were made with respect to the categories (which also included reports of normal appearance, designated negative) and features, with respect to four proposed hypotheses of causes. These were tidal, low–angle illumination, magnetic tail and solar flare particles that produced magnetic storms on Earth (and therefore reached the Moon). Both numbers and their percents were considered.

Data are presented in tabular and graphical form. In the latter, it is easier to see behavior among the categories and among the features as to influences. The data are compared within boundary conditions for each hypothesis **–** whose periods are not commensurate, as they overlap at times. Overlaps were compared and showed that almost 70% of observations overlapped at least two hypotheses introducing confusion as to dominating influence.

Analyzing by numbers, the tidal and low–angled illumination hypotheses were about equal in dominance. When ratios of observed to expected percents within boundaries

were compared, which is a truer indication of influences, only one hypothesis (low–angle illumination) was dominant. Thus sunrise–sunset conditions render escaped gas or dust particles more visible because of the longer light path.

These results, coupled with the very low number of features reported (~200) among the >30,000 visible in telescopes; reported with anomalies; their non–random distribution – in contrast to the randomness of impact features; association with volcanic features (maria, dark–floored craters, domes, and sinuous rilles), imply that the Moon is not totally inert, but degasses independently from external influences (as does the Earth). This is supported by the detections of recent emanations, moonquakes, internal heat and compositional layers by instruments on the Moon and those on board during orbits of the moon.

Key Words: LTP, instrumentation, behavior, categories, features, distribution, tidal, low–angle illumination, magnetic tail, magnetopause, bow–shock front, solar.

I. INTRODUCTION

Human interest in the night sky and its objects, especially the Moon, antedates written history. Other species are cognizant of the Moon, particularly the canines. The author (WSC) from childhood was fascinated with astronomy, especially the Moon. This carried her into astronomical education, the U.S. Naval Observatory, and ultimately NASA's Goddard Space Flight Center, and assignment to research on the Moon.

Comprehensive search of the literature of old and contemporary books and journals by astronomers, particularly selenologists who observed the Moon over decades brought to her attention these anomalies in lunar features. These observers came to know the lunar features and their aspects over all phases of lighting conditions. In these publications, references to and citations of their own and others about temporary, phenomenal events here called Lunar Transient Phenomena (LTP) were noted and described. Events lasted from fractions of a second (flashes) to seconds, minutes, hours, and even, occasionally days, averaging about half an hour. Finding so many in the literature from many professional astronomical and scientific societies' journals, a collection of them were started in 1960, and a catalog of observations from 557-1978 A.D. was published (W.S. Cameron, 1978). The extension to that is in progress, to be published later.

Interest grew among astronomers and geologists and intensified by our effort to go to and land on the Moon. These LTP origins and causes became important, especially for those confirmed or permanently recorded, for safety in landing purposes and geological interest.

Other methods of observations besides visual were through photography, photometry, spectra and polarimetry, all of which recorded anomalies. As these became published, hypotheses of causes of the phenomena of several kinds of manifestations were proposed. For purposes of analyses of these, the catalog of 1468 entries included auxiliary data (and the extension one likewise). The first six of the reports were made before the invention of the telescope in 1610 A.D. and are therefore by naked eye (and a few of these since). The auxiliary data needed for analyses and interpretation included: observer's names, location, observing experience, equipment parameters such as, kind of telescope (refractor or reflector), aperture, focal length of the objective and eyepiece used, sky conditions, features and their lunar coordinates, dates and time of observations, (converted to U.T. by W.S.C. and descriptions of the phenomena.

Several papers appeared with analyses producing somewhat different results and conclusions. These involved a tidal effect, first proposed by J. Green (1964), followed by J. Burley and B. Middlehurst (1966), B. Middlehurst and P. Moore (1968), Cameron and Gilheany (1966) and W.S. Cameron (1972, 1977, 1978) the latter author considered other hypotheses as well.

II. OBSERVATIONS

The data consist of reported observations of temporary anomalies seen on the Moon over a period of 1.5 millennia! They contain visual (sometimes independently confirmed) and permanently recorded observations of the LTP. The permanently – recorded can be consulted at leisure and many times.

Prior to 1960 the favored origin for lunar features was volcanic. After 1960 the favored interpretation for origin was impact. The features are: craters (sizes 1-290 km), circular maria (large dark volcanic areas 200-1200 km), irregularly–shaped dark areas larger than the circular ones, mountain ranges surrounding the circular maria (probably impact features) and isolated ones, (1-40 km), domes (volcanic), rilles (valleys) which are linear [radius of curvature (ROC) @ 1000 km tectonic], arcuate (ROC-100 km, probably related to impact) and sinuous, ROC 1 km (volcanic) which are quite rare as are domes. In many of the sinuous rilles there are inner sinuous rilles, especially those on or just off of the volcanic Aristarchus plateau. The sinuous rilles have distributions similar to the LTP sites. The largest sinuous rille is Schroeters Valley and it with Herodotus and Aristarchus have contributed ~1/3 of all LTP. There are over 30,000 craters that can be seen in the telescope, but only ~200 of them have ever been reported for LTP at least once. Half of these have been reported twice or more, many of them with many reports. Schroeter's Valley, hence often abbreviated to SV, in the Cobra Head part (origin of the valley) is the only place in which physical change has been seen (J. Greenacre, oral pc to WSC).

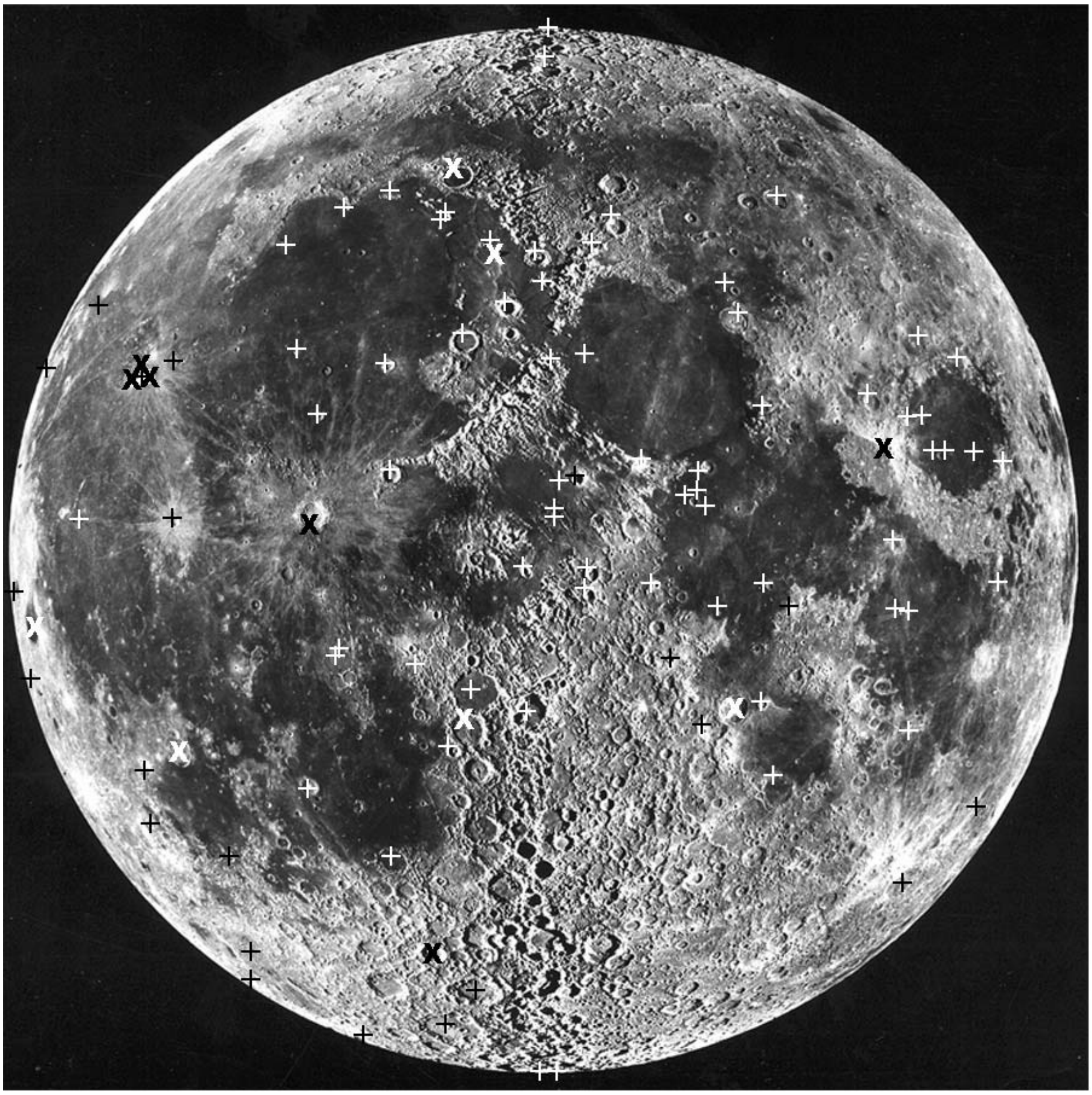

Plate I. A Lick Observatory composite photograph of the Moon. Superimposed on it are the 100 features that have been reported more than once as exhibiting Lunar Transient Phenomena (LTP). The twelve features discussed in the text are marked by the bold "**X**" symbol, while the rest are plusses (+).

Image by permission of UCO/Lick Observatory.

Plate I "Distribution of 100 LTP sites on the Moon" shows the location of these 100 features, hence their distribution. The large **X'**s are for the twelve features discussed in the text. It is evident that they are non–random, contrary to that of all impact craters, which are randomly distributed. The LTP are almost exclusively in or near the dark areas – especially the maria. Through the lunar probes and manned landings the dark material has proved to be volcanic. Their non–randomness and association with the volcanic dark areas implies that LTP may be manifestations of internal activity, mostly mild degassing, but at times more intense, localized bursts.

The LTP observations fall into five categories and the negative (normal aspects) are also analyzed. These five categories are Darkenings, Brightenings, Reddish, Bluish and Gaseous. A dozen features comprise ~60% of all observations. These were analyzed as well as the categories. The full list is provided in the Appendix.

III. OBJECTIVES

The objectives of this paper were to analyze the LTP observations for their distribution over the Moon. Correlations with the various hypotheses proposed for external causes for the manifestations and whether the different categories were influenced by different mechanisms. The dozen most frequently reported features also were analyzed in the same way to establish whether they or parts of the Moon responded to various influences differently and to each other. Among them they were particularly compared with those grouped together if less than 10° apart in longitude (where forces would act stronger than in latitude). Comparisons with distributions in age, and tidal phase, comparisons of ratios of percents observed to those expected under the boundary limits of the hypotheses – a more accurate and perceptive notion of real correlation than with just numbers; tests for bias in observations; overlaps of boundaries of the hypotheses as the periods were not commensurate; and comparisons of features with categories were analyzed. The data are given in tabular form and their graphic depictions.

IV. METHODS OF OBSERVATIONS

In addition to the above mentioned types of observations, for the Association of Lunar and Planetary Observers, as Lunar Recorder for LTP the author devised a program for measurements of albedo compared with normal ones as given by T. Elger, in Goodacre (1895). Elger's albedo chart (1895) gives examples of features that represent each half step of his chart from 0 (black shadows) to 10 (central peak of Aristarchus – the apparently brightest spot on the Moon).

The system set up was for observers to observe the listed features at each half step of the chart at full Moon, recording in some fashion, a matching gray scale. This could be done by pencil shadings, photographic gray scale wedge, one made by the observer by exposing film at various exposure times, superposition of pieces of unexposed film, comparison to a full Moon paper print, or neutral filters.

Features were assigned to each observer in the program in order to cover all 100 LTP sites in the program; four LTP, one non–LTP, for comparison, one permanent nearby plain, also for comparison, and a seismic epicenter, as given by Y. Nakamura (1976). Records of their observed albedo (by using their constructed scale with which to match the observed gray), over all phases, of several chosen permanent points that were always measured, were made in a record book and copies were sent to the Recorder on a regular basis, such as monthly. At least two measurements per night, separated by at least 15 minutes were to be made. This program covered 20 years for the first Recorder (WSC), now continued by D. Darling and David Weier. It was the first one from which the frequency of LTP occurrences can be obtained. Before this, only positive events were reported with no indication of how many observations had been made with no anomalies. Here all observations were sent. These were mostly visual observations. There were, however three professional systems of rotating neutral and color filters devised, two under the auspices of NASA, one of which WSC was the federal monitor. This one was the Trident Moon Blink system of the U.S. Naval Academy, Annapolis, MD (Cameron and Gilheany, 1966). This system used a cathode luminescence and rotating filters (4-12 rps). It had provisions for four other instruments to utilize the incoming light to each instrument, including camera, spectrograph, photometer, and polarimeter. Differences in brightness between two colored filters would produce a blink. Another somewhat similar system was designed for A. Hynek at Corralitos Observatory, also using rotating filters, but at a much lower speed and between each, the screen took 10 sec. to clear so the blink effect really was less effective than the Trident one. The British Astronomical Society (BAA) devised a simpler blink system. One of the latter was used by WSC. Five of the Trident ones were dispersed among groups. Several anomalies were recorded on film over a period of five years.

Observers separated by large distances and even different countries independently confirmed many observations in the catalog. McCord, Scarfe and others recorded anomalies using photometric methods also Cameron (1978) did on a spectrum. There are over 100 reports in the catalog that were permanently recorded among the 1468 events listed, and many more are in the extension (as yet unpublished) but those data are included in this paper. Apollo missions had instruments and experiments (both orbital and landed) that recorded various anomalies. Orbital ones on Apollos 15-17 detected radon and polonium (both short–lived radiations) in several areas on the lunar surface. Aristarchus and the plateau on which it is located was one. This area provided about 1/3 of all LTPs. Their short half–lives <100 yrs., show that lunar emissions are still occurring. The LACE and SIDE surface experiments registered bursts of atmospheric molecules denser than normal, one at least had atomic mass near that of water, which was not released from the orbiter. The seismometers left on the Moon have recorded Moonquakes ~10,000/yr with Richter scale magnitudes usually of 1-2, but one was over 4. Due to funding decreases the receivers were shut down in the late 1970's.

V. SAMPLES OF OBSERVATIONS

Many reports were of flashes in features on the Moon. Possibilities of cause could be: (1) Earth's atmospheric meteors crossing the field of view (FOV) of the telescope, (2) meteors striking the Moon large enough to produce light that could be observed from Earth or (3) volcanic eruptions, some of which may have lightning, as in terrestrial eruptions. Except for the volcanic possibility, the others could and should occur randomly across the lunar surface, yet many have been seen in the same features at many other times! Plato and Grimaldi both have many reports of flashes in them (Cameron, 1978). These then, cannot be by chance meteors. Astronauts, orbiting the Moon have seen some. T. Mattingly, CMP on Apollo 16 (1972) when orbiting the Moon alone, saw a flash on the backside of the Moon, below his horizon. "That could have been a meteor there." H. Schmitt on Apollo 17, when all three astronauts were orbiting the Moon (before landing) saw a flash in Grimaldi (1973, 1997). When questioned, privately at a meeting about his observation, he said, "unfortunately, that he was dark–adapted at the time so could not say whether or not it was due to a cosmic ray flash in his eye" (an experiment on board for the astronauts).

These observations were recorded on the mission tapes. Because of many previous recorded flashes over time in Grimaldi, Schmitt's report was probably a real LTP.

Apollo 11 Astronauts, N. Armstrong, B. Aldrin, and M. Collins, were alerted to a phenomenon being reported by many observers on Earth occurring in Aristarchus. They were asked to look at it on the next orbit. They did and saw a brightening in the NW wall of Aristarchus at the same minutes of time that two observers in Bochum, Germany were reporting such activity in it! This constitutes a confirmation and was not a terrestrial atmospheric effect since the astronauts were at the atmosphereless Moon.

Spectra of events have been obtained in Alphonsus by N. Kozyrev of Russia (1959, 1960, 1962, 1963, 1964). One absorption spectrum out of 14 taken on one night of seven features and two comparison spectra at the limb on two plates, one hour apart were taken by the author. The absorption line, in Plato, appears on only one of the two plates taken that night. Over 300 spectra were obtained over an almost two year period and this was the only anomaly found in inspections. Kozyrev's anomalous spectra were in Nov. 1958, and Oct. 1959 in Alphonsus and three different times in Aristarchus within a week in 1961. He started his program after reading of D. Alter's discovery in the Lick Observatory photos taken in the 1930's.The anomaly was in Alphonsus showing obscuration of half of its floor. This was in the 1950's while going through the Lick photos. He then started a program of photography using red and blue filters in succession each night. He mentions this in his book (Alter, 1979). It was about two years later that he obtained a similar anomaly in Alphonsus. He used the Lick 36-in refractor. It also took Kozyrev about two years to get his first one in Alphonsus, using the 50-in Pulkovo Observatory's reflector. Kozyrev's dispersion was 30 Å/mm. W. Cameron, inspired by his results started a spectral program on about 20 features using a dispersion of 107 Å/mm. Using the 6-in spectrograph on Goddard's 36-in reflector in Greenbelt, MD. Kozyrev identified C2, N2, and carbon bands, all emission, in Alphonsus, and H2, C2, and N2 emission bands in Aristarchus. The absorption line obtained by Cameron is a blend at her dispersion, at 4908 Å contains H2 in the blend. The anomaly was in Plato. D. Harrison (1970) in 1961 obtained, visually, an absorption band in Alphonsus at 4910±40 Å. Cameron's error was ~4 Å, so probably he observed the same one as Cameron did in Plato. Z. Kopal and T. Rackham (1964) photographed the Moon and caught brightenings at Copernicus, Kepler and Aristarchus on the same plate (Kopal 1966). R. Wildey and H. Pohn (1964) over a one and a half year period photometered 25 features over 25 nights. On more than half the nights two runs were made. Study of their data by Cameron (1980) found several anomalous measures. One night in particular, the brightest of their 25 features was in Mare Crisium (site of several LTP), a dark area, which varied in brightness between the two runs that night both of which surpassed Aristarchus'!

VI. EXPLAINABLE TYPES OF PHENOMENA

There are three types of phenomena reported that probably can be attributed to terrestrial effects and these would be deemed non–intrinsically lunar phenomena. In the analyses below the ALL data included these, but not the best (*) data.

(1) Star–like points have frequently been reported, even by the eminent W. Herschel (1787) who saw ~150 during a lunar eclipse. The author also saw ~½ dozen during a lunar eclipse (her 1st LTP). Later, during the Apollo 13 watch she saw ~20 points (among the myriads of bright craters) all located centrally on the illuminated crater's rims under excellent sky conditions. The next night, none were to be seen in them or any other ones, under similar sky conditions as the night before. One would expect to see them at the

same point in the illuminated crescent but physically located slightly moved around the rim. They were points under low magnification and smaller telescopes, but became patches of brightness under high magnification, and larger telescopes, where the same amount of light was spread out over an area instead of a point. Thus these are probably related to aperture and magnification. Another brightness phenomenon often reported is of short–term variations (seconds) often seen during early, crescent phases of the Moon and in the ashen light–Earthshine on the Moon. The author proposes that these are terrestrially produced by clouds on the limbs of the Earth as seen from the Moon, though some may be from the atmosphere over the observer. The former clouds would likely not be solid but intermittent in motion (such as mackerel sky or buttermilk sky) where alternate clear and cloudy conditions would obtain. They are the influence that affects the darkness of a lunar eclipse.

The third type is a two–colored phenomenon in which red is on one side of the rim of a crater and blue is on the opposite side. L. Fitton (1975), after a series of such observations were reported by members of the British Astronomical Association (BAA) and confirmed over a week's period, found that there was an atmospheric temperature inversion over the British Isles at that time which acted as a prism. He predicted that one would see red on the south rim and blue on the north rim of a bright crater on a darker background (e.g., Aristarchus). The reverse in colors is red on north and blue on south of a dark crater on a lighter background (e.g. Plato). Many reports have such conditions. This explanation probably does not hold for single colors reported. An assiduous observer, C. Bartlett (1967) frequently reported bluish–violet in some features, mostly in Aristarchus. It is likely that he, and others were more sensitive to blue than those who reported white conditions. These two–color reports also are in the ALL data but not the (*) data.

There were many reports of phenomena that implied a medium was involved, even an atmosphere. Examples were extension of cusps beyond the poles, non–instantaneous occultations and aurorae. The author discounted these and weighted low as not probable because of the known extremely low density of the lunar atmosphere (one trillionth of Earth's). This can now be questioned in view of recent professional observations that detected a tenuous atmosphere on the Moon composed mostly of sodium, but aluminum and potassium were also found (A. Sprague, etal 1998 and F. Graham 1995, 1998). Perhaps especially denser than normal bursts of degassing occurred and were observed in the dark sky above the limb of the Moon. Sometimes more than one type of phenomenon in the same feature or in others at the same time was reported. In those cases they were listed in each category in the analysis.

It was also noted that only about one dozen features contributed over 60% of the total of all observations. These dozen, mostly craters, were: Proclus, Theophilus, Piton (an isolated mtn.), Alphonsus, Plato, Tycho, Copernicus (can be seen with the naked eye due to its large concentric ray system, nearly at the center of the full Moon), Gassendi, Aristarchus (apparent brightest feature on the Moon), Herodotus, Schroeter's Valley (largest in overall dimensions of the sinuous rilles and it has a smaller sinuous rille within it wandering from side to side in the larger one). The latter two are combined in the analyses, often abbreviated H/SV, and Grimaldi, in order from east to west (IAU astronautical).

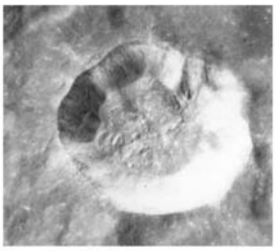

A. PROCLUS
Apollo 17 Hassleblad FR.23046

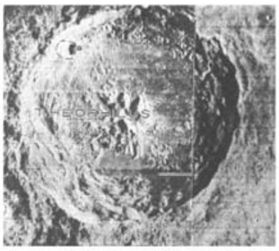

B. THEOPHILUS (GAZETTEER)
LO IV 77-2, 84-2

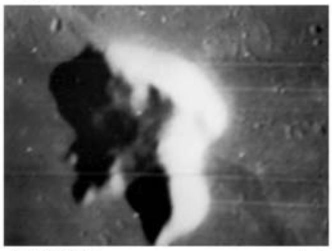

C. PITON
LO IV 115-2

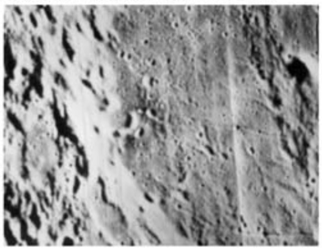

D. ALPHONSUS
LO V 119M

E. ALPHONSUS FLOOR
LO V 116-1

F. ALPHONSUS' C.P.
LO V 116

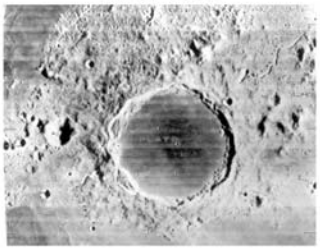

G. PLATO
LO IV 127-3

H. TYCHO
LO V 125M

I. TYCHO'S FLOOR
LO V 125

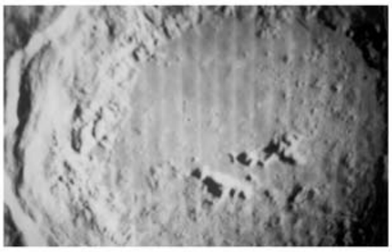

J. COPERNICUS
LO V 151M

K. (OBLIQUE) COPERNICUS' FLOOR
LO II 162

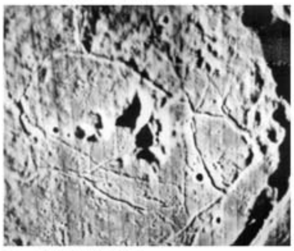

L. GASSENDI
LO IV 143-2

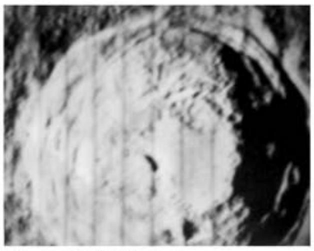

M. ARISTARCHUS
LO V 201M

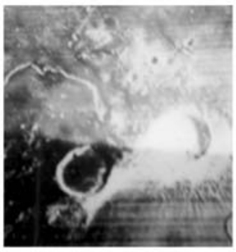

N. ARISTARCHUS, HERODOTUS
SCHROETERS VALLEY
LO IV 150-3

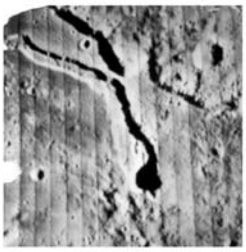

O. SCHROETER'S VALLEY

LO V 203M

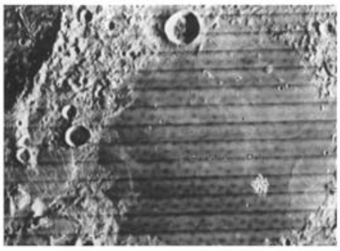

P. GRIMALDI (Gazetter)

LO IV 168-3

Plate II. A montage of lunar photographs courtesy NASA'S National Space Flight Center (NSSDC) cropped from frames of the Lunar Orbiter series of spacecraft, for the 12 features analyzed and discussed in this paper. The spacecraft is designated as LO, followed by the Orbiter number (I, II, III, IV, V) and the frame number in Arabic. There were two cameras aboard each spacecraft, one for medium (M), and one for high magnification in which the section of the frame is given in Arabic numbers, e.g. LO IV 163-3. Each photo is labeled A-P. Some of these photos from the originals were not in the author's possession and were taken from the Gazetteer--NASA SP-241, titled Atlas and Gazetteer of the Near Side of the Moon, prepared by G.L. Gutschewski, D.C. Kinsler, and E. Whitaker.

Plate II "Selected Features for Analysis" shows each feature, taken mostly from the Lunar Orbiters. The above samples among other data support the contention that the Moon is not inert or inactive but still degasses gently most of the time, but sometimes, perhaps more violently as well as sustaining impacts.

The data were analyzed in both divisions of categories and features with respect to lunar age, tidal anomalistic phase, within boundary conditions of four hypotheses, and percents of observed and expected (within those boundaries) and the ratio of percents of observed to expected, which is the best gauge as to external influences.

Plate II: (A) Proclus (30 km). Note the eccentric hills on the floor of this impact crater that has directed rays (not seen here as the sun angle is too high). (B) Theophilus (100 km) showing its central peaks (cps). These are seen to be fractured parts of a single large peak. Some have summit craters (scs). (C) Piton is an isolated mountain with a large sc. Note that a mare ridge approaches it and is interrupted by it, as seen in the upper left and lower right. All photos here are oriented with north at the top. If extrapolated through the mountain, it passes under the sc, suggesting that Piton is a volcanic feature. (D) Alphonsus (128 km) shows part or the W wall and part of the floor with its central ridge and cp with sc. The Ranger 9 spacecraft crashed into the crater–taking pictures till it landed. This feature is the source of many LTP, several of which are spectra. (E) Part of the floor of Alphonsus showing several of the dark–haloed craters here. There are others on other parts of its floor, all of which are the sources of the surrounding dark material, which is volcanic therefore they are volcanic craters. All have rilles coming from or into them. (F) This shows Alphonsus' central peak well which is superimposed on the central ridge that crosses the whole floor, the only crater on the Moon with such a feature! There is a small sc barely seen, as part of it is in the shadow. (G) Plato (100 km) shows its dark floor. The vent or cp is absent. There are no breaks in the walls for mare material to invade, so it has its own source (vent). Note also, two sinuous rilles starting on its outer flanks, upper right and lower left. Sinuous rilles are volcanic features also. (H) Tycho (86 km) is an impact crater with the longest ray system on the Moon (not seen here). Both cps have scs. (I) Shows part of the floor of Tycho showing numerous domes and rilles, some with scs, others with fissures and slumped material (upper right). (J) Copernicus (89 km), near the center of the Moon is the center of a large ray system visible to the naked eye. It shows the W rim and the aligned cps some of which are like breached cones. Also the East side of the floor has numerous domes, some with scs and some with directed blast ejecta. These are probably volcanic. Compare Tycho's and Copernicus' cps in Plate II, both are same–sized craters (86km and 89 km respectively). (K) Oblique view of Copernicus (89 km N–S, 27 km E–W). At the middle right edge is a positive crater with a cp, which has an sc. This is the shape and size of Nova Rupta in the Valley of 10,000 Smokes, Alaska (similar in origin?). (L) Gassendi (88 km) showing cps with scs and many fissured valleys. (M) Aristarchus (46 km) is the brightest impact crater on the Moon and the source of several hundred LTPs over as many centuries. On the NE floor is a ring of domes, several of which have scs. Other features on the floor also suggest subsequent volcanism after the impact as most of the above features do. (N) Shows the three adjacent features, Aristarchus (46 km), Herodotus (38 km) and Schroeter's Valley (10 km x 190 km) all on the volcanic Aristarchus plateau. These, together, supply ~1/3 of all LTP reports. (O) Enlarged section of Schroeter's Valley whose upper part, known as the Cobra Head, is the source for the large sinuous rille. The large rille has an inner rille that meanders on the floor of the big one and its source is a hill with summit crater located in the Cobra Head. (P) Grimaldi (219 km) dark–floored crater showing its dark floor with several domes in the northern part, some of which have sc's (right side of the photo). It is near the western limb of the Moon. It is the source of several flashes, one of which was seen by the geologist astronaut on Apollo 17.

VII. DIVISION OF DATA

In the perusal and study of the large body of observations (2254 in ALL) it was found that the observations fell into five categories (six when negative = normal are included). These categories were designated as: 1.) Brightenings – flashes, increases in brightness (albedo), brighter than normal; 2.) Darkenings – dimming, darker than normal; 3.) Reddish – color phenomena in the warm part of the spectrum, from yellow – infrared; 4.) Bluish – color phenomena reported in the cool part of the spectrum, from green – violet; 5.) Gaseous – those that implied a medium was involved – misty, clouds on them (lunar), dissipation, movement of clouds (lunar), color of shadow other than black, e.g. gray, brownish, or lighter. The medium could be gas and/or dust. Both the American and Russian landlers detected dust above the ground. The American Surveyors detected it above the horizon, calculated to be ~1 meter above the surface. Russian Lunakhods detected It ~1 km above the surface. The latter perhaps may have been seen from Earth at times of very low sun angles (near the terminator conditions).

VIII. HYPOTHESES OF CAUSES

As early as the mid 1960's hypotheses were offered as to possible external causes of these phenomena. There were several with variations.

1.) Terrestrial tidal effects on the Moon, which would be at least six times stronger than the tidal effects on Earth from the Moon, even in its solid parts. The first to suggest this was the geologist J. Green (1964). He had studied and measured water and oil well levels, finding that they changed in time and were correlated with the Moon's orbital motions, a tidal effect. The strongest effects were at apogee and perigee. The Moon's orbit is more eccentric (elliptical) than Earth's (~ 0.055 vs. 0.017 respectively) mainly due to the Earth's mass that is 81X the Moon's. Thus tides on the Moon would be expected to raise the lunar surface to ~125 cm vs. ~22 cm on Earth by the Moon. From Green's analyses of the well data he proposed that tidal effects on the Moon should be strongest near the extreme apogees, and weakest at the smallest perigees. The varying eccentricity of the Moon's orbit has a cycle of 14 months and the true anomalistic phase (Φ), measured from perigee – perigee varies, averaging 27.7 days, varying from 25-28.5 days. The synodical period of revolution (new Moon – new Moon) is 29.5 days and the sidereal month (vernal equinox to vernal equinox is 27.3 days. The difference arises because the Earth has moved in its orbit by about 30° and the Moon has to catch up to it for new Moon again. In the analyses here a period of 28.0 days was used in the statistics because the Moon is not easily observed within 1.5 days of new Moon.

2.) B. Middlehurst adopted the anomalistic phase (new Moon to new Moon) and used intervals of 0.10 Φ (Burley and Middlehurst, 1966). The true anomaly which includes the eccentricity of the lunar orbit, and is more accurate, is calculated by the horizontal parallax (π) formulae:

$$\text{Cos } E = \{(1/\pi_a)+(1/\pi_p)-(2/\pi)\} / \{(1/\pi_a)-(1/\pi_p)\}$$

$$V° = E° + 5.89 \sin E°$$

$$\Phi_\pi = V°/360$$

π_a = horizontal parallax of apogee,

π_p = horizontal parallax of perigee,

π = parallax of time of observation,

$V°$ = true anomaly in degrees,

$E°$ = eccentric anomaly in degrees,

Φ_d = anomalistic phase in days and can be approximated by,

$$\Phi_d = (D-P_1)/(P_2-P_1),$$

D = date of observation (UT),

P_1 = date of perigee before observation,

P_2 = date of perigee following date of observation,

Φ = true anomalistic phase.

The Φ_d is divided by 360°. This assumes that the lunar orbit is circular. The maximum difference between Φ_π and Φ_d is 0.10 Φ, but the difference is usually small.

IX. BOUNDARY CONDITIONS FOR EACH HYPOTHESIS

The hypotheses proposed have limits that can be expressed in boundary conditions at the Moon where they would be effective. Below are those chosen boundaries, which are dictated by the proposers as effective.

Low–angle illumination includes three hypotheses Greenacre and Barr (1963), Sidran (1968) and Blizard (1968). The boundaries considered were 1). SR and SS combined ≤±2.0 days. SR ≤+2.0 days, and SS ≤–2.0 days in a period of 28.0 days (lunation) for statistics but ages are from the 29.5 day synodic period.

For tidal effects (Burley and Middlehurst (1966) and Chapman (1967)), the interval of 0.10 of the anomalistic phase Φ_d was adopted. In this paper Φ_d (rather than Φ_π) was used, as there were more data for it than for Φ_π. The maximum difference between the two is 0.10 Φ, which is rarely found. Thus correlation would be ≤±0.10 Φ_d for perigee (P) and apogee (A), thus ≤20% for each and 40% for both combined. The average anomalistic period is 27.7 days.

For Magnetic Tail effects, ≤±2.0 days FM for MP, and ≤±3.5−4.5 days FM for the BSF for a period of 28.0 days were used. This is a generous limit for the BSF, as A.G.W. Cameron (1964) gave none. Particles should arrive from solar flares at the Moon not more than an hour before or after reaching the Earth (which would be a more accurate limit). These particles take about 36 hours to reach the Earth from the Sun (Lincoln 1965). The magnetic data give measures of the Kp index (Bartels 1962) chosen here in 3h intervals. Kp ranges from 0-9 for each day of the month, and a graph of values for each 3h daily for each month for the year. Sudden commencements of magnetic storms on the Earth (when observed) are indicated. Magnetic storms may last for several hours to over a day. Sc's and ms's when sc is not observed were noted. A value ≥Kpmax6- and ≤±0.5d ms as limits for correlation were chosen. The number of magnetic storms in those indices over a 20 year period (almost two sunspot cycles) were made and it was found that the percentages for correlation were 9% for ≥Kpmax6- and 18% for ms's ≤±0.5day. Percentages for magnetic tail and low–angle illumination correlations are 14%, 7%, and 7% and 14% respectively.

X. PRESENTATION OF OBSERVATIONAL DATA

The data have been manipulated in several ways and are displayed in tables and pictorially in graphs. The tables cover many aspects of the observations, but their constructions are quite similar. The observations are analyzed in the following ways: (1) for all data under categories (Tables 1, 2 & 3 and Figures 1 & 2 (a)) and (2) for all data of individual features (Tables 1, 2 & 3 and Figures 1 & 2 (b)). Tables 1 and 2 considered numbers of observations, under (a) and (b) with respect to lunar age and tidal anomalistic phase respectively. The construction of most of the tables is similar in format. After numbers of observations in the first two mentioned formats the data are given in numbers with respect to tidal anomalistic phases' boundary conditions (Tables 2a and b). Tables 2a and 2b give numbers of observations vs. boundary conditions for each hypothesis. Tables 4a and 4b give analyses for the percentages that the numbers represent and compared with percentages expected under the boundary conditions if they were evenly distributed which would be that there were no external influences. The ratio of observed to expected O/E are given. These tables are the most revealing as to real correlation with the proposed hypotheses. Table 5 gives the number and percentages of overlaps in boundary conditions of each category. Bias for one type of observations (near terminator) was examined. Finally, Table 6 gives comparisons of the categories vs. the dozen features, both for each feature, across each category, and for each category along each feature taken from Tables 1 and 2. Beneath Table 6, in Figure 3, the percent's data are shown graphically for easier comparison of the behavior of features across the category and for each feature along each category.

The layouts for these tables are as follows: under categories e.g. Table 1a there are four columns for each category which give all numbers of observations over each lunar age (0-0.9) regardless of weight or value e.g. ALL, with Col. 1 (All), Col. 2 (+) gives all numbers of confirmed/permanently recorded observations, Col. 3 (*) the chosen best data and Col. 4 (*+) the conf/perm for the chosen best data (Col. 3). The highest number of observations in each Col. is in boldface and underlined, for easier comparison of behavior among the categories. In the lunar age table the average boundary ages for the magnetic tail's magnetopause (MP), and the bow–shock front (BSF) are indicated in the left margin; thus that hypothesis can be evaluated as well as the lunar ages that have the most observations. The average phases are also indicated in the left margin. Total numbers of observations are given at the bottom of each column.

For features (Table 1b) the same divisions are given except that instead of four columns, there are two (for space considerations) with two rows for each column where the upper row is for All and +, while * and *+ are given in the lower row. Here, for features, the average age of sunrise (SR) → and sunset (SS) ← for each feature is indicated by a small arrow in the first Col. of each feature. The days of darkness for each feature are grayed. This allows comparison to the low–angle illumination hypotheses as well as the lunar age and magnetic tail hypotheses.

Other information given are: lunar selenographic coordinates for each feature – below the name {progressing from IAU east to west across the Moon), those craters with dark floors have black ovals above the name (the rest are bright features). The dark floors are of volcanic material. Features that are close in longitude (<10°) are grouped by brackets at the top of the table. Their behaviors would be expected to be similar; the largest numbers of observations are bold–faced and underlined, for easier comparison among the features, especially those grouped together. Totals are at the bottom.

The graphical forms (Fig. 1b) depict just the 1st col. upper row (All) solid graph (–), and the 2nd col. upper row (+) dashed lines (–x–) from Table 1b. The total number for each day's point is at midday. Totals are at the right of the legend in the figure. Also shown are the times that the features are in shadow (night) as light gray areas. Average sunrise age $\overline{\mathrm{SR}}$, local noon on the feature $\overline{\mathrm{LN}}$, and sunset $\overline{\mathrm{SS}}$ are indicated. Vertical lines are drawn at average full Moon $\overline{\mathrm{FM}}$ heaviest solid line, magnetopause $\overline{\mathrm{MP}}$ lighter solid lines, and bow–shock front $\overline{\mathrm{BSF}}$ as long–dashed lines. Totals of observations and lunar coordinants are at the right side as are the brackets for the close–in–longitude groups. The average first quarter $\overline{\mathrm{FQ}}$ as ☽ average $\overline{\mathrm{FM}}$ as ○, and average last quarter $\overline{\mathrm{LQ}}$ as ☾ are indicated.

The tables for numbers of observations for categories, and for features vs. the anomalistic phase (Φ_d) for the tidal hypotheses are labeled 2a and 2b respectively, with average perigee $\overline{\mathrm{P}}$ and apogee $\overline{\mathrm{A}}$ between heavy horizontal lines (the pertinent places for the tidal hypotheses) are emphasized.

The tables for number of observations for categories and features vs. hypotheses' boundary conditions are 3a and 3b respectively and have the similar format as in previous tables. Negative (normal aspects) data are included, but only for All and + as they were not rated for value.

Tables for ratios of percents of observations to expected in boundaries of hypotheses for categories and features are Tables 4a and 4b respectively for All and +. The four columns for each category, and each feature are (1) for All and + numbers in the upper row and for * and *+ in the lower row, (2) their percents of the total numbers given in the column for totals (% obs), (3) percents expected under evenly–distributed observations in the boundary limits (% Exp) and (4) the ratio of observed to expected O/E. The latter gives a better perspective on the real correlation with each hypothesis. The same format is used for features (Table 4b.). As in all tables the largest numbers of observations of the first row in any 1st col. are bold and underlined, while the largest ratio O/E (col. 4) is bold, italicized and underlined. The same holds for the second row of the 1st col.. These are the most significant information of each category's data. There were sufficient numbers of observations under * for Aristarchus and for * and *+ for Plato. These data are in the last two features columns, headed XXX.

The boundaries of the hypotheses (as the periods are not quite commensurate) overlap. Table 5 presents the numbers of observations for the various overlapped boundary conditions. The first section is for Tidal vs. (A) Magnetic Tail, (B) Low–angle Illumination, and (C) solar. The second section is for Magnetic Tail vs. (D) Low–angle Illumination, and (E) Solar. The third section is for Low–angle Illumination vs. Solar (F), thus all combinations are covered. The overlap of observations is given for each No. Col. and the largest of these is bold and underlined for each column. Below, the total numbers of observations of each case are given. Below this total is given the largest number's percent in each case. Thus, the percentages of the largest numbers show how much overlap occurred in each section. The largest number's percentage for each case is bold and underlined, with the highest percentage also italicized.

Finally, Table 6 and Fig. 3 give the numbers of events and percents for Features vs. Categories. The table can be read in two ways: (1) for each category, the total of the events for all eleven features is given in the Categories Total column; (2) for each feature, the total of the events for all five categories is given at the bottom of each Features' column.

The first col. for each feature gives the numbers of observations (No.), and the second col. gives the percentages (%) of that number (1) upper %, with respect to the Category totals at the right, and (2) lower %, with respect to the Feature totals at the bottom. The highest number in the upper % for each feature column is bold and underlined, and for the lower % the highest percent for each category row is bold, italicized and underlined. The two groups close in longitude (<10°) are bracketed.

In Figures 3a and 3b the percents data are shown in two graphical forms for easier comparisons of behavior. Figure 3a for the percentage of a feature in the category and figure 3b for the percentage of the category in each feature. The solid–lined one (–) is for the upper percentages in the column (3a), and the dashed–lined (**–**x**–**) is for the lower percentages in the column (3b). Here too, the groups are bracketed. Again, the dark–floored craters are indicated by dark ovals over their names.

XI. DISCUSSIONS AND INTERPRETATIONS OF DATA

Table 1a "Numbers of Observations for Categories vs. Lunar age", whose format was discussed above, in the section on presentation of data, shows the data at each day of lunar age from 0.0d, new Moon (NM) through all the phases to (NM) again (29.5d). The four phases' ages are labeled at the left margin. Besides the five categories discussed before, there is a column for negative (Neg.) observations which were when the features showed normal aspects of behavior. The first Col. is a typical light curve of illumination throughout a lunation (NM**–**NM, 0-29.5) days.

[Table 1a]

To facilitate interpretation of all these data, there are four cols. in each category except Negative, which has data just for All and its confirmed/permanently recorded (+) data. The largest number in each col. is bold and underlined and forms the salient points for interpretation. These indicate the behavior of each category and therefore permit comparisons between them. The hypothesis that can be addressed here is that of the magnetic tail's two boundary conditions, namely within the magnetopause (MP) and at the bow–shock fronts (BSF), both entering and exiting, indicated at the left margins of Table 1.

For details in Features, the best viewing dates are from ages 3-11d. Full Moon is best for dark and bright terrain contrasts (the fanciful figures of the man in the Moon, lady in the Moon. Gibson girl. etc.) plus the ray systems.

Looking at the bold numbers one notes differences in behavior among the categories. Some categories have maxima at the BSF entrance: ALL * & *+; Gaseous All, * and *+; and Reddish all four divisions; but Neg. also has both its highs there. One might expect Neg. to behave opposite to the positives (all other categories). Thus there are three positives and one negative category that behave similarly at the BSF entrance. Within the MP there are ALL All and Bluish's All. There are none at the BSF exit. Darkenings and Brightenings depart from the others, with Brightenings All and + considerably different from everyone else. Reddish is the only one that has all divisions showing the same behavior. Brightenings is nowhere near any others in its All and + data except for ALL's +. This is not too surprising as Brightenings has the largest total of observations (totals at the bottom) of any category, 60% of ALL. Most of the observations fall in the 3-11d ages, but observations are found over the whole lunation!

In many cases the other divisions (+, * & *+) differ from the All data of their same categories. ALL differ considerably, as do Darkenings, and Brightenings, and Gaseous somewhat. Note that the All numbers are nearly equal from ages 5-15d. Fig. 1a "Numbers of Observations for Categories vs. Lunar Age" shows this dramatically.

[Figure 1a]

The data in Table la can be depicted graphically and this is found in Fig. 1a. This figure has the 1st and 4th cols. of Table 1a (All and *+) graphed. The points are placed at midday but cover the whole day from 0.0-0.9. At the bottom, in the ALL category, is a representative light curve for the Moon during a lunation (0.0-29.5d) so that comparisons may be made between the categories and lighting conditions. At a glance one can see differences in behavior between the categories and departures from the light curve (LT in Table 1a). There are no two that behave the same way in the All data. The closest are ALL and Reddish. There is more accord among the best's conf/perm (*+) where five of the seven (ALL, Brightenings, Darkenings, Reddish and Bluish) are similar. The *+ data are small in number, but have more weight for validity. None follow the light curve well, falling rapidly after FM. Note that all categories have observations covering a whole lunation (from 0.0-28.0d). Several phenomena were seen during solar eclipse totality – seen on the Moon's dark disk.

Most categories have peaks. Some are less than the highest in the MP between the light solid vertical lines, which includes FM (one heavy vertical line). These are ALL (its highest), Brightenings, Darkenings, Bluish, and Gaseous. Note that Gaseous has high numbers from 3-18d, then they taper off. ALL has its highest peak at FM as does Bluish. Negative is practically a mirror behavior to the others after the BSF entry, but similar to the others before that (up to 11d).

The best data (*+) often depart in behavior from their All data in the same category, e.g. Brightenings, Darkenings, and somewhat ALL. Negative and Gaseous have highest peaks at the BSF entry. Only Negative has a small peak at BSF exit. The results among the categories suggest a possible magnetic tail influence.

[Table 1b]

Table 1b "Numbers of Observations for features vs. Lunar Age" is constructed similarly to Table la except that data for * and *+ when not zero are given in the second, lower row for each feature. Under the feature name the lunar coordinates are given in the IAU aeronautical convention and the features progress from east to west. Dark ovals above the name indicate those features with dark floors (volcanic). At the top are brackets that enclose those features that are <10° apart in longitude (in which the hypothetical influences are more effective than in latitude). At the left margin, the boundaries for the MP and BSFs of the magnetic tail are noted. Also small arrows in the first col. for each feature indicate the average day of age that sunrise and sunset (SR and SS respectively) occur thus comparisons can be made with the low–angle illumination hypotheses as well as age and magnetic tail.

The All bold numbers go down stepwise in age reflecting when they are in sunlight. In many cases the bold, underlined salient points occur at or near average sunrise (SR). Ones that don't are Proclus, Tycho and Grimaldi (in that it has three maximums, one of which is at SS. In a few cases the + data do not agree with their All. Examples are Proclus, Alphonsus, Plato, and Copernicus (considerably for the last two). In some cases the highest are equal at different ages.

In the 1st bracketed ones, Plato, and especially Tycho depart from the others (Piton and Alphonsus). In the 2nd bracketed ones, Aristarchus and its very close companions

Herodotus/Schroeter's Valley behave similarly, but are slightly off from Gassendi. However, all three come a day after SR (but within the boundaries of the low–angle illumination hypotheses). Three are at or near the BSF entrance, which is also when SR occurs on them (thus overlap of two hypotheses). Two are within the MP and are not near their SR. Grimaldi's are in the waxing crescent phase, which is night for it! One of Grimaldi's is at the SS in the waning crescent ages. Many of the conf/perm + and best * and its *+ generally agree with their All data. These relationships are better seen in Fig. 1b

[Figure 1b]

Figure 1b "Numbers of Observations for Features vs. Lunar Age" depicts the data in Table lb for All and + for all features, and in the case of Aristarchus *+ is included. Vertical lines indicate the boundaries of the $\overline{\text{FM}}$ (heavy solid), $\overline{\text{MP}}$ (light solid) and $\overline{\text{BSF}}$ (dotted) ages. The **grayed areas** are when the feature is in darkness with the boundaries indicating average sunrise $\overline{\text{SR}}$ and sunset $\overline{\text{SS}}$ respectively. Average phases are shown at the bottom border and top border, which are NM ●, FQ ☽, FM ○, and LQ ☾. Average local noon $\overline{\text{LN}}$ is indicated within the graphs. Those features <10° of each other are bracketed at the right side. Dark ovals at the name indicate a dark–floored crater, and total numbers are also given.

The behavior of the features differs in the trends as can readily be seen by noting the bold, underlined numbers, which are the highest numbers. Except for Grimaldi, they show peaks at or near $\overline{\text{SR}}$. Alphonsus, Tycho, H/SV and Grimaldi show small peaks at $\overline{\text{SS}}$. The latter may actually be quite significant as observing times are in the early morning hours, for the western features, which for most avocational observers are very inconvenient, thus seldom made. Proclus and Tycho, peak in the MP. Gassendi has its highest peak near the MP entrance. Only Grimaldi has a high at the BSF exit. Nearly all have been seen in the waxing ashen light before $\overline{SR}$ and a few in the waning ashen light. Thus there are correlations with both low–angle illumination and with magnetic tail, the only two hypotheses that can be addressed here. The former one is perhaps more dominant. Note also that the observations for all the features cover the whole lunation period, not just the favorable times for observing.

[Table 2a]

Table 2a "Numbers of Observations for Categories vs. Tidal Anomalistic Phase (Φ_d)" for All, All +, *, and *+ data addresses numbers of observations in the tidal hypotheses' boundaries at 0.10 Φ_d for each category, and includes the categories of Negative and Middlehurst's data. As in all tables the highest numbers in each col. are bold and underlined. They give the trends in behavior. Negative has data just for All, and All+, and Middlehurst has just All, the only quantity she discussed in her paper (Burley and Middlehurst, 1966). Perigee $\overline{P}$ and apogee $\overline{A}$ are where tidal activity should be strongest. These rows are emphasized by being enclosed in heavy horizontal lines. These then should be the focus of attention. Contrastingly, the Φ_s at 0.25 and 0.75 should be minima. Of the 27 cols. among the eight categories, 12 are at P, and only one at A (Darkenings). Negative has a max at the 0.25 min. and four maxes in the positive categories are at 0.75, the other expected minimum!

Some observational descriptions included more than one category and those features were included in the data for each category described. This is the case for all tables and figures on categories in this paper and likewise in the figures.

Six out of the eight categories shown have at least one division with max at P. Darkenings *+ at A and Negative are the exceptions. This might be expected for Negative.

Reddish has three of its four divisions at 0.75 Φ_d (though one is tied with P). The other one is at 0.4 Φ_d (near A). It also has a high (but not highest) at P.

There is, apparently a strong correlation in tidal effect on All data, but it is effective at P, and is near minimum at A. This is enigmatic for tides should be equally effective at both P and A as it is on Earth that has two tides per day, both at closest to the Moon and 12 hours later when it is farthest from the Moon. These of course, pertain to all locations on Earth as it turns. Later it will be seen that its boundaries overlap the other hypotheses' boundaries, with the highest being with low–angle illumination's.

[Figure 2a]

Figure 2a "Numbers of Observations for Categories vs. Tidal Anomalistic Phase (Φ_d)" shows the data of Table 2a for cols. 1 and 4 (All and *+). Vertical lines emphasize P and A. Totals are given at the right side. An idealized curve for a real tidal behavior is on the bottom graph (light solid).

In all the data the strong peaks at P are evident. The only strong (though less than the one at P) peak at A is for Middlehurst data, for which the total is only 145 observations. Even Middlehurst's curve departs from the idealized one, though is the most conformable of all the categories. Most of the categories show a general dip after P for half a period (P–A) and a broad high in the last half period (A–P). Negative is generally opposite to most of the positives, but conforms very much to the Bluish. Gaseous does not conform to the others, it has three peaks; the 0.4 and 0.0 (1.0) $\Phi_{d,}$ and are equal, and the 3rd (at $\Phi_d = 0.7$ – near expected min) is almost as high. The + data (conf/perm) generally conform to the All data. The opposite behavior of the Negative to that of the positives supports the correlation with P but one still has the problem of lack of their correlation with A.

[Table 2b]

Table 2b "Numbers of Observations for Features vs. Tidal Anomalistic Phase (Φ_d) gives the data of the dozen features that were discussed in Table 1b but for the tidal anomalistic period phase (Φ_d). It is constructed similarly to Table 1b Perigee (P) and apogee (A) are indicated at the left margin and those significant rows are between heavy horizontal lines to emphasize these salient areas for the tidal hypotheses. At the top, those features <10° apart in longitude are bracketed. The dark–floored craters are indicated with dark ovals below their names, and their lunar coordinates are given below that. Totals for each col. and row are given at the bottom. There are two rows in each col., the upper one is for All and +, and the lower one is for * and *+. The highest nos. (significant) are bold and underlined and those will be discussed as they show the behaviors without searching through the whole table for those for comparison of behaviors. It can be seen at a glance that the features don't all agree, even those within brackets that would be expected to be similar in behavior. Ten rows, out of 44 (~1/4) agree and are at P. There are two features (Aristarchus and Plato) that have * data there, Aristarchus's * and Plato's *+, which however is tied at two other phases (0.4 and 0.6 <Φ_d), while the Aristarchus * data have ties at P and 0.9 Φ_d.

There are three out of 44 that have max nos. at A, all of which are * data. For the four bracketed features, only one (Plato) has max at P (*+). In the three other bracketed features they all agree, with maxes at P in the All row, except for H/SV's All +. Aristarchus's * is also at P but its *+ is at 0.9 Φ_d, and H/SV has ties at P, 0.40, and 0.9 Φ_d, and its All at P and 0.9 Φ_d. Gassendi's All + max is tied at P and 0.3 Φ_d and its All at P and 0.9 Φ_d. In general, the features are pretty much scattered in their behavior throughout the anomalistic phases. Plato has three of four divisions the same at P, but its *+ is tied with

0.4 Φ_d and 0.6 Φ_d. Gassendi has three of its four divisions' maxes at 0.3 Φ_d (near expected min). These results are more easily seen in graphical form in Fig. 2b.

[Figure 2b]

Figure 2b "Numbers of Observations for Features vs. Tidal Anomalistic Phase (Φ_d)" is constructed similarly to Fig. 1b for features for All and + data. Plato and Aristarchus had sufficient data to include their * data. Values for the four points after P (1.0) = 0.0 are repeated so that the trend around P can be seen.

Here, in the All data the departures among features are seen more readily. Gassendi through Grimaldi have similar trends near P, but depart elsewhere. Grimaldi's peak is at 0.7 Φ_d, an expected minimum! Note particularly between the bracketed Aristarchus and Herodotus/Schroeter's Valley, which are very close in longitude and latitude. In the 1st 7/10ths they are about opposite. In the other bracketed ones there is almost opposite behavior, though Alphonsus and Tycho are somewhat similar. Proclus differs considerably from all others, except near P, and is almost a mirror image of Theophilus and Alphonsus. Only two, Aristarchus and Grimaldi have a peak at P, all others are just before or after P except Theophilus, which has a minimum there. Plato has high nos. from 0.4-1.0 Φ_d a broad high with max. at 0.7 Φ_d (an expected min. in the tidal hypotheses). In general, the + data trends are similar to their All data. The * data for Aristarchus and Plato also conform to their All.

[Table 3a]

Table 3a. "Numbers of Observations for Categories in Boundaries of Hypotheses" depicts the four hypotheses to be considered, viz. tidal, low–angle illumination, magnetic tail, and solar. The boundary conditions are as follows: for data with respect to P in the tidal, the limits are ≤±0.10 P (perigee) and likewise for A (apogee), and for P and A combined (P/A). Low–angle illumination, sunrise (SR) and sunset (SS) are the pertinent limits which are, respectively ≤+2.0d SR, and ≤-2.0d SS, and ≤±2.0d SR/SS. For magnetic tail the limits are ≤±2.0d FM (MP), and ≤±3.5d-4.5d FM (BSF). The one–day limit at each BSF is quite generous, but was chosen by the author, as none was given by A.G.W. Cameron. As there are separate hypotheses for the MP and BSF they were not combined. For solar (magnetic particles ejected from solar flares that reach the Earth), the limits chosen were from the Kp index, which is an indication of the strength of the magnetic field flux at the Earth (and Moon). The limits chosen almost always are connected to magnetic storms. There are magnetic storms sometimes generated at lower indices that range from 0-9, but these are rare. The limit chosen is ≥Kp max 6-. Kp indices are 3h sections from 0-24h for a day. The max for the day of observation was picked. Anything with Kp 6- or higher was counted for each day of the LTP date. The other limit is for the occurrence of very high activity indicating the Earth was experiencing a magnetic storm, usually the start is observed on Earth, known as a sudden commencement (sc). Sometimes the start was not observed at any station around the world. The designation ms (magnetic storm) includes the sc's. The limits for the ms are ≤± 0.5d ms. These two are not combined. All four divisions under each category are given.

As before, the largest numbers at any limit in the col. is bold and underlined. It is immediately apparent that most maxima are found at P/A (perigee and apogee). This is not surprising as it is the widest boundary condition encompassing an average of 5.5 days around each, so that 11 days out of 27.7d (average period) are involved, a percentage of 40%. These will be considered later. Of the 26 columns (78 nos.), 13 have maximums at P/A. There are 11 cols. at SR/SS. For magnetic tail there are 26 cols. (52 nos.), one col. is at MP and one at BSF (Negative). It is almost a toss–up as to a main influence between tidal and low–angle illumination. As will be discussed later, the periods of each hypothesis are not commensurate, but are near so and thus overlaps occur. Only two categories Darkenings and Bluish show all four divisions of data at P/A, ALL has two. The table indicates that magnetic tail and solar effects are very little or not active.

[Table 3b]

Table 3b "Numbers of Observations for Categories in Boundaries of Hypotheses" is constructed similarly to 3a except that * and *+ are given in the lower row. Considering the upper row, for All and **+**, for the 22 cols., eight (~1/3) had maxes at P/A, five of 11 features have at least one there. Eleven cols. have maxes at SR/SS and three at MP. For the lower row, six out of 22 cols. are at P/A, 12 at SR/SS, and one (under Grimaldi) is at MP.

The behavior of the close in longitude bracketed ones shows differences in behavior, (yet one would expect them to be similar). In the first group, only Plato had all four divisions at P/A. The other three features were at SR/SS. In the second bracket, all three had some of their maxes at P/A for the upper row, but only Aristarchus had all four divisions (both rows) there. The other three divisions, for Gassendi and H/SV were at SR/SS. Tycho, Copernicus, and Grimaldi had their All **+** maxes at MP.

Thus, the two operative hypotheses were tidal and low–angle illumination, though three features had maxes in the MP.

[Table 4a]

Table 4a "Categories – Ratios of Percents of Observations to Expected in Boundaries of Hypotheses" gives data for All and *****+**. The first col. is No. of Observations, 2nd col. gives the percent (%) of that no., the 3rd col. gives the expected % and the 4th col. gives the ratios of the observed to the expected (O/E) percents. The latter col. is the most significant as to correlations, and is set off by heavy vertical lines. The expected % is that which would be expected in the boundaries if there were no external influences, thus would be evenly distributed throughout the periods. Again, in each Category, the highest numbers are bold and underlined. The highest ratio is bold italicized and underlined for each row. Regarding the 1st col.'s upper nos., all but Reddish and Negative have maximums at 0.10 P/A. Reddish and Negative are at ≤±2.0d at SR/SS. The lower row has three of the seven categories at P/A, and three at SR/SS (ALL, Gaseous and Reddish), and one (Negative) at BSF.

Looking at the ratio col. O/E – upper row all categories have maxes at SR! The lower row shares six of the seven at SR. The 7th one (Negative) is at BSF! It is also the highest ratio of all (8.1) which is 8X what would be expected. The min. ratio is 2.7, still almost 3X expected for ≤+2.0d SR. Note that all the ratios of P/A are near 1.0 with the highest, in Darkenings, at 1.2, or only 20% above expectation.

The result is that the low–angle illumination hypotheses are the dominant ones, and the effect is at SR, which favors Blizard and Sidran as to cause (UV stimulation to escaped gases or contained gases and/or minerals). If gases are there it is the long path of sunlight that renders them visible to observers on Earth.

[Table 4b]

Table 4b. "Features – Ratios of Percents Observed to Expected in Boundaries of Hypotheses" for eleven features is similar to Table 4a and gives data for All and **+**. Two additional cols. labeled XXX give * and ***+** for Plato and * for Aristarchus, both of which had sufficient data at these boundaries for significance (***+** was not done for Aristarchus). Again, the 1st row is for All data and the 2nd row is for their **+** (conf/perm) data. Also the 1st col. for each feature gives the numbers of observations in which the highest number in that col. regardless of hypotheses is bold and underlined. Column 2 gives the percentages of col.1 data with respect to the total given at the bottom of the col. for each hypothesis. Column 3 gives the expected percentages under even distribution, which would be expected if no external influences operated. Column 4 gives the ratios of the observed % to the expected % (O/E). This col. is set off with heavy vertical lines, as it is the most significant quantity and gives the real influential correlation. The highest ratio for each row in the col. is bold italicized and underlined.

Table 4b is derived from Table 3b for the numbers of observations (Col. 1) within the boundary conditions of each hypothesis and their divisions. This table converts the observed numbers in Col. 1 to their percentages with respect to the totals at the bottom of each hypothesis, thus column 2 is the observed percent. It is desired to compare them to the percents of <u>expected</u> percents within the boundaries if there were no external influences, therefore distributed evenly throughout the period of each hypothesis. These are given in Col. 3. Column 4 (emphasized by vertical lines) gives the ratio of the observed to expected percents (O/E). In the first column the highest number of observations down the hypotheses is made bold and underlined. Data are given for All (Row 1) and **+** (Row 2) which are respectively all observations, and the confirmed/permanent records of All. To summarize the results, considering Col. 1 numbers, they are tabulated below with each division of each hypothesis.

	Tidal			Low-angle Illumination			Magnetic Tail			Solar
	P	A	P/A	SR	SS	SR/SS	MP	BSF	Kp>6-	MS
Row 1 (All)	0	0	6	1	2	6	1	0	0	0
Row 2 (**+**)	1	0	1	7	1	6	3	0	0	1

Thus for All (Row 1) 6 had the most observations at perigee and apogee, and SR/SS also had six while SR had one and MP had one.

Row 2 (**+**) had seven for SR, one for SS, three for MP, and one (tied with P/A) for magnetic storm (MS). Observations with highest numbers were nearly equally divided between tidal and low–angle illumination largest boundary conditions, but SR (sunrise) had the most (7) of all divisions for the conf/perm observations.

This shows that two hypotheses were equally dominant or operating on the data while magnetic tail was weak and solar magnetic storms had little effect on observations.

Highest ratios Col. 4 comparing percents of observations to those expected within the boundaries. Looking at Col. 4 (ratios) for the highest ones' out of 13 in Row 1.

	Tidal			Low-angle Illumination			Magnetic Tail			Solar
	P	A	P/A	SR	SS	SR/SS	MP	BSF	Kp>6-	MS
Row 1 (All)	0	0	0	12	2	1	1	0	0	0
Row 2 (**+**)	0	0	0	7	1	1	3	0	0	0

In this most significant comparison, the low–angle illumination hypothesis is most dominant with none in the tidal and three in magnetic tail's magnetopause (Speiser 1967). It should be noted that in the tidal hypothesis 40% of all observations should be seen in the boundaries if there were no tidal effect. The ratios (O/E) in the tidal are close to unity or in other words about what would be expected if no tidal effect.

Therefore the results of the most significant data (O/E) strongly support the low–angle illumination hypotheses, especially near SR. The numbers data lend some support for a tidal effect but only at P and are deficient at A. A few, especially in the **+** seem to be affected by the MP of the magnetic tail, but not the BSF.

A look at the bracketed features and their behaviors in their ratios shows near unanimity in each group, all having high ratios at SR, which is rather specific – not at the broadest conditions of the low–angle illumination hypotheses. These results suggest that conditions near sunrise are good for detecting anomalies, probably because of the longer path of sunlight through any medium (at favorable viewing times).

It's been mentioned before that since the periods of the different hypotheses are not commensurate then their boundaries overlap and more than one hypothesis obtains, at times. Occasionally all four overlap! If the observations mention more than one kind of phenomenon, it was included in each category mentioned.

[Table 5]

As a result of curiosity as to the role that percentages and pertinence to interpretation of the overlaps might play, Table 5 "Category Overlaps of Boundary Conditions" was constructed. Each of the hypotheses' boundary conditions is compared with the other. The columns (A–F) are arranged in sections – tidal, magnetic tail and low–angle illumination (indicated by brackets), so that each hypothesis is compared with the other. The boundaries are listed under each title above. E.g. in the first col. and the 1st overlapped set is magnetic tail's magnetopause MP ≤±2.0d FM vs. perigee (P) ≤±0. 100P. The observed no. (No.) gives the number of overlaps (163). At the bottom is the total number of overlaps (1792) that the tidal boundaries were overlapped by the magnetic tail elements with the highest percentage number (bold and underlined) to the total, below them. The next col. considers the tidal vs. the low–angle illumination boundaries. The third group under tidal is tidal vs. solar boundaries. Of course the highest nos. will be the broadest combined boundary conditions. The highest percentage is also italicized.

The largest percentage for any condition is 16%, and that is for tidal and magnetic tail overlapping. However, two others each had 14%. Surprisingly one of these is low–angle illumination vs. solar! The least, at 5%, was for magnetic tail vs. solar. All percents added up amount to 68% of all observations that included at least two conditions, which were responsible. These results say that the magnetic tail did not have much influence on the solar particles that were bombarding the Moon! This contradicts the results from analyses of energies of solar particles not being sufficient to excite luminescence to a brightness that could be seen from Earth! Tidal alone overlapped all other hypotheses 41% of the time.

XII. TEST FOR BIAS FOR LOW ANGLE ILLUMINATION

Such a test was made for the 11 features analyzed in this paper. Seven of the 11 had the most frequently reported ages near sunrise (SR). The exceptions were: Tycho for sunset (SS), Aristarchus for full Moon (FM), Grimaldi for ashen light (it was in darkness, especially the waxing phases) and Proclus had equal nos. for ages 3d (SR), 11d LN – (local noon), and 16d (SS). Thus Proclus had highs at both limits for low–angle illumination plus LN.

The percentages of occurrence near the terminator (SR and SS) varied from 10% for Alphonsus to 29% for Aristarchus. Expected percents (no external influences) would be 7% for SR and also at SS, or 14% for both. Thus there may be bias for the terminator, mostly for SR, as SS occurs for many of these features after FM, when observations are much fewer because of the lateness in the night (early morning) for viewing. These are small percentages compared to all observations, which extend throughout a lunation (0-28d). Several lunar surface events were seen during solar eclipses! Some were recorded then. The largest quarterly numbers are found from FQ–FM, especially for ages ≤±3.5d FM. Thus, in a whole lunation, there really is little bias for the terminator. Those boundary conditions favor the detection of LTP if there were a medium involved.

[Table 6], [Figures 3a & 3b]

Table 6 “Features vs. Categories” shows the variations in numbers and percents for each feature vs. each category. The highest category number in the first column of each feature is shown bold and underlined. There is one number in the 1st column. – (No.) and two percentage figures in the 2nd column – (%), for each feature. The upper % is the percent of this Feature down each Category. The lower % is the percent of the Category along the Features.

It shows that the category with the majority of highest numbers and therefore the highest % in the upper row was Brightenings (6), followed by Reddish (3), two in Gaseous, none in Bluish or Darkenings and that individual features varied among themselves.

The feature with the highest percentage of a category (lower row) is bold, italicized and underlined. Aristarchus had the highest percentage in each category. Its contribution to Bluish of 66% was the highest % of any category. Thus almost 2/3 of its LTP were bluish. For comparison among the bracketed features, following the underlined figures, one can see that the features respond differently from each other in general, even in the brackets. In the upper row for the 1st bracket (indicated at the top) two, Plato and Tycho, are similar and are of Brightenings. Piton is for Gaseous. Alphonsus is for Reddish. In the other bracket all are different. Gassendi’s high is in Reddish. Aristarchus is in Brightenings. H/SV is in Gaseous.

Figure 3 “Plots of Percentages in Table 6” graphs those percentages given in the % cols. of Table 6. The graphs are, respectively, (3a) solid line graph is the upper row of data and gives the percentage of each category that is found in a feature. The dashed graph on the right (3b) plots the lower row of data and shows the percentage distribution of the features found in each category. Here it can be seen that the features behave erratically, even among the bracketed ones (shown at sides of graphs as thick solid vertical lines) although 3 of 4 are similar, Piton differs. Their dashed graphs differ from each other, therefore responding differently to external influences. This is quite noticeable between Aristarchus and H/SV, which are so close. Some may behave similarly in three categories then depart from the other two. Alphonsus and Gassendi behave similarly, in both phase and degree. The features responded differently as to kinds of phenomena.

XIII. SUMMARY

There are many kinds of evidence that support the probability that the Moon is not yet inert, but does emit gases. Mostly it is gentle degassing, but probably at times there is inhibition, leading to collection, then final emissions of denser bursts, sufficient to produce changes in aspects and luminosity to be seen from Earth. Observations have ranged from naked eye to very large telescopes and their auxiliary equipment. Some have been permanently recorded, providing proof that anomalous, temporary conditions have occurred. These are here referred to as Lunar Transient Phenomena (LTP).

Several hypotheses for origin or cause have been proposed, which include low–angle illumination, tidal, magnetic tail and solar particle bombardment effects on lunar surface features and materials.

The observations (>2200 over 1.5 millennia) could mostly be classified into five categories, plus reports of normal (Negative) conditions for features. The five categories are: Brightenings, Darkenings, Reddish, Bluish and Gaseous. The latter encompass any suggestion that a medium, (gas or dust) was involved. Some observers reported manifestations covering more than one category, e.g. bright, reddish and gaseous. In the analyses these were considered in each category.

It was also found that about one dozen features contributed over 60% of all reports! The number of features reported at least once was about 200. These are out of >30,000 features observable in telescopes! Of these 200, ~100 were reported more than twice and many were reported many times, under different lighting aspects. Their distribution over the lunar surface is decidedly not random, unlike that of the craters, mostly of impact origin, which are randomly distributed over its surface. There are many features though, that are volcanic in origin, and some of these have been reported as LTP. Many of the large impact craters have had subsequent volcanism. Examples of lunar volcanic structures are: the circular maria's fillings, domes, different from the lunar mountain ranges and sinuous rilles (valleys). Spacecraft instrumentation has recorded bursts of materials in the form of very recent radon, polonium, and material with the density of water.

With the advent of hypotheses for causes it was considered important to analyze the reports with respect to the boundary conditions for each category and for each of the dozen features most frequently reported as anomalous in aspect. It was found that these dozen features contributed more than 60% of all, half of them 50% and one (Aristarchus) ~1/3.

These data were analyzed from several tables. Tables that contained data for analysis in the categories were labeled (a), and the same kinds of data for the features were labeled (b). Constructions for the tables are quite similar, containing data under the headings ALL (all data regardless of value or weight of the observation), those ALL data that were confirmed or permanently recorded labeled (**+**). Choices were made from reports considered to be most probably real events, not explainable by several terrestrial conditions that existed at the time, which might have produced the effects. These are labeled * and their conf/perm ones are ***+**.

The tables present the observations vs. several conditions. Tables 1a & 1b present the numbers of observations vs. lunar age for categories and for features respectively. Tables 2a & 2b give numbers of observations vs. the tidal anomalistic phase (Φ_d) for categories and features, respectively. In the same manner, Tables 3a & 3b give numbers of observations included in the various boundary conditions for each hypothesis. Tables 4a & 4b present the numbers of observations with the observed and the expected percents for each hypothesis, and the ratios of the observed to expected O/E in Col. 4. Here, expected percents are what would be expected within those boundaries if there were no external forces operating, and therefore should be evenly distributed over the periods.

Table 5 presents numbers of observations of overlaps of the boundaries of the various hypotheses. Percents of the largest numbers from the totals are given.

Table 6 derived from Tables 1 & 2, presents the numbers (Col. 1) and their percentages (Col. 2) of the tables. The upper row of percents is for each feature across the categories, whose totals are at the bottom and the lower row for each category along the features with totals at the right edge. The highest percentage for each category among the features (upper) is bold and underlined and the highest percentage for each feature across the categories is bold italicized and underlined.

Figures 3a and 3b present the data from Table 6 graphically for the percentages for easier comparisons of behaviors of each feature and each category.

A bias test for observations at the terminator (mostly sunrise–SR), but also for sunset (SS) as at these times more detail can be detected, was made.

Summarizing interpretational results from the tables follows. Table 1a "Numbers of Observations for Categories vs. Lunar Age" where the age containing the most observations is emphasized in each col. and the boundaries of the magnetic tail are labeled for comparison and for correlation, so that behavior can be assessed. The Negative (normal aspects) observations are included. It is found that four of the six categories, (1) ALL's * and *+, (2) Gaseous' All, (3) Reddish's *, and (4) Negative's had highs at the bow–shock front (BSF) entrance of the magnetic tail. One would expect the Negative to be opposite the positives. In the tail of the magnetopause (MP) ALL's All and Bluish's had highs' there, while Darkenings and Brightenings depart from all the others. Most of the highs' numbers over the categories were in the 3-11 day ages when lunar detail can be made out. Figure 1a shows the All and **+** trends in behavior more easily and the differences between the categories stand out. No two categories are completely in synch. In general the conf/perm (**+**) data conform to the All, but Brightenings and Darkenings depart from all others.

Table 1b "Numbers of Observations for Features vs. Lunar Age" shows that the low–angle illumination hypothesis can also be assessed at sunrise (SR) and sunset (SS) as these average ages are indicated by small arrows in the All Col. and the magnetic tail average ages are also indicated at the left margin. The underlined bold numbers show that there are strong relationships with SR for most features. Proclus and Grimaldi do not show those relationships. Four of the features' maxima are in the magnetopause of the magnetic tail (MP) rather than at SR. The features Herodotus and Schroeters Valley combined (H/SV) has highs in its **+** data at SS. Grimaldi has several equal maxes, one of which is at SS, but none at SR! Figure 1b "Numbers of Observations for Features vs. Lunar Age" shows that Tycho differs from its three neighbors (<10° apart in longitude). Three of the four in the 1st bracket (that group features close in longitude) have rises at SS. Only Tycho has a peak though not the highest in MP. In the 2nd bracketed set Gassendi differs from Aristarchus and H/SV, but only the latter shares a rise at SS.

For interest, those craters with dark floors (volcanic) are indicated with dark ovals near their names, and the lunar coordinates of each feature are given as well as the totals of observations.

Table 2a “Numbers of Observations for Categories vs. Tidal Anomalistic Phase Φ_d” has the pertinent boundary conditions for P and A in the tidal hypotheses emphasized by heavy horizontal lines. All but Darkenings and Negative have at least one division of the data at perigee (P), but only one – Darkenings has a peak at apogee (A). Middlehurst’s Col. is there and has a lesser peak at A. ALL and Reddish have at least one division high at 0.7 Φ_d where a minimum would be expected. The data support a tidal effect at P but not at A where minima occur for most. Theoretically the tidal effect should be equally strong at P and A.

Figure 2a “Numbers of Observations for Categories vs. Tidal Anomalistic Phase Φ_d” shows these results for the All and *+ data. None of the graphs are similar to Middlehurst’s and each differs quite a bit from each other, but all except Negative, (which has a slight dip there), show maxes at P and lows at A. Compare this with an idealized tidal curve shown in the bottom graph. In general the *+ data conform to their All data.

In Table 2b “Numbers of Observations for Features vs. Tidal Anomalistic Phase Φ_d” looking at P and A (also enclosed by heavy horizontal lines), six of the features have at least one division at P. Plato has two, Aristarchus has three, Gassendi has two at P. H/SV and Proclus have at least one division at A, but H/SV has two highs at 0.4 Φ_d. The other five features’ maxes are scattered throughout the Φ_d period phases.

Figure 2b “Numbers of Observations for Features vs. Tidal Anomalistic Phase Φ_d” depicts the data of Table 2b for All and All +. Two features, Plato and Aristarchus had sufficient data to include * (best data). Only Aristarchus has its max trend at P. Grimaldi has a peak there, but not the highest, Grimaldi, Gassendi and H/SV have broad peaks at 0.9-1.0. Proclus has a broad one at 1.0(0.0)-0.1. Note that Aristarchus and Grimaldi have double humps in the half period from A–P while Theophilus has them in P–A. The features in the first bracketed group of four differ from each other, although 3 are somewhat similar. In the 2nd bracketed group, Aristarchus and H/SV (very close to Aristarchus both in longitude and latitude) behave quite differently. Only Theophilus and Piton do not show declines from P–A while Proclus is low except near and at P. Aristarchus and Grimaldi decline from P–A, both have the double–hump at 0.7 and 1.0 (P) Φ_d. Proclus is unique in behavior compared with the others.

Table 3a. “Numbers of Observations for Categories in Boundaries of Hypotheses” contains data for all divisions, All, **+**, *, and ***+** for all except Negative for which just All and **+** are given. All but Reddish and Negative had at least one division at perigee and apogee (P/A) limits. Darkenings and Bluish had all divisions there. All and Gaseous had at least two divisions at SR/SS, Reddish had all divisions there. Two categories, Brightenings and Negative, had at least one division in the Magnetic Tail. Brightenings had its **+** at MP and Negative’s **+** at BSF, but Brightenings All was at P/A and Negatives All was at SR/SS. None were under solar.

There were 13 divisions (out of 26) that responded to the tidal effect under the widest boundary condition of all hypotheses (P/A). A near number (11) is at the low–angle illumination at SR/SS, while two were under magnetic tail effects. Thus All’s and *’s **+** at P/A (6) and All’s and ***+**’s at SR/SS (5) data were influenced almost equally by tidal and low–angle illumination. All Darkenings and Bluish were at tidal, while Reddish was all low–angle. These suggest that at least two categories correlate with two different causes of external effects.

Table 3b. “Numbers of Observations for Features in Boundaries of Hypotheses” for upper row All and **+** (which is the confirmed/permanently recorded) had 8 highs out of 22 divisions at P/A (Perigee and Apogee combined boundary conditions), 11 of 22 at upper row SR/SS (Sunrise and Sunset combined boundary conditions), 3 of 22 at MP (magnetopause part of magnetic tail) boundary condition and none at either Solar boundary conditions.

For * and ***+** (best data and its conf/perm data) there were 6 (of 22) at P/A, 12 at SR/SS, one at MP, and none under Solar. Thus 14 of 44 divisions were at P/A, 23 of 44 at SR/SS, and 4 of 44 at MP and none under Solar.

Comparing the bracketed features < 10° apart, three of four (1st bracket) almost totally agreed at SR/SS while all four of Plato’s had maxes at P/A. The second group differed in divisions of three had at least one max at P/A. Aristarchus had all four divisions there. Thus there is much less agreement among the three features, two of which (Aristarchus and H/SV) are only 1° apart in longitude and latitude so should respond equally to any external influences. Gassendi and H/SV correlated more closely.

The features correlate similarly with the categories, both correlate strongly with two hypotheses, viz. tidal and low–angle illumination, but many more divisions correlated with SR/SS than with tidal (23 vs. 14 features) for P/A, while they were almost equal (11 vs. 13) between the two hypotheses in categories. These data suggest that possibly two hypotheses influence events. Magnetic tail had only a slight influence.

Table 4a. “Categories – Ratios of Percents of Observations to Expected in Boundaries of Hypothesis” treats the data in a different context in that it compares observations (and their percentages from the totals) within the boundaries of each hypothesis to that which would be expected were they not affected by any external influence. Thus, even or random distribution is expected. Maximum numbers of observations (No.) are highlighted as before by bold and underline. The max (O/E) in col. 4 (between heavy vertical lines) is bold, underlined and italicized.

When the max nos. are considered, (1st col.), with two rows, upper for ALL and **+**, the lower for * and ***+**, it is found that five of the seven categories had maxes at P/A for ALL and **+** (upper row) and three of seven for * and ***+** (lower row), or a total of 8 of 14 divisions at P/A. There were two of seven in upper row for SR/SS and 3 of 7 for lower row SR/SS, thus 5 of 14 divisions at SR/SS. There were none for ALL and **+** (upper row) of Magnetic Tail (MP) and one for * and ***+** (lower row) at BSF of Magnetic Tail. There were no maxes under Solar.

When the ratios are considered (4th col.) [these are much more significant for true correlations] the results are entirely different. The max <u>Nos.</u> were mostly at P/A (the widest consideration in which 40% of all observations should be) in <u>O/E</u> there are no maxes at P, A or P/A. For the <u>O/E</u> maxes of ALL, they are at SR. For the ***+** 's, six of the seven are at SR. The exception is for Negative at BSF of the magnetic tail, both in number and ratio, which should behave differently from the other categories. Thus all of the positive categories correlate most strongly with low–angle illumination's SR. It is noteworthy that the ratios under tidal are near 1.0, the highest being 1.6, and this is at P, yet P/A has the largest numbers. Table 1b and Fig. 1b showed these. At A (apogee) there are very few numbers and ratios, much less than expected. These results intimate that at low–angle illumination conditions, LTP are rendered favorable for detection. Observations are scattered over a whole lunation and if lumped together in bins of weekly groups, the majority are found around full Moon, which is surprising as only contrasts in albedo (brightness) can be readily seen. Inner details cannot be distinguished otherwise.

Table 4b. gives data for All and **+** except for Plato and Aristarchus which also have * and Plato also has ***+**, and is similar to Table 4a. First, considering the cols. of No., 7 of the11 features (All) have at least one division with max at P/A (four of which have both divisions there). For *, both Plato and Aristarchus have maxes at P/A and also Plato's ***+** (Aristarchus was not analyzed for ***+**). Proclus' All and **+** are at P/A.

For **+**, four have maxes at P/A. For all the rest of the features, four have maxes at SR/SS. Thus, in numbers the features are equally divided between tidal and low–angle illumination.

Considering the ratios for All, considerable differences occur from numbers. Ten of the eleven features have their maxes at SR. The one different (Proclus) has its max ratio at MP! For **+**, six of eleven have maxes at SR. Dissenters are Proclus with max at P, Theophilus at SR/SS, Copernicus' All and **+** differ: All is at SR and **+** is at MP. Again low–angle has the preponderance of max ratios. P has one (Proclus) and MP has four.

Boundary conditions among the hypotheses overlap as given in Table 5 (Category Overlaps of Boundaries of Hypotheses) because of incommensurate periods between them. When this happens it cannot be determined which hypothesis is responsible. There are cases where all four boundary conditions overlapped, confusing the interpretation all the more.

This table investigates just how much this occurs. Each hypothesis' set of boundary conditions was investigated vs. each boundary of the other hypotheses. Numbers of overlaps are given. The totals of observations are given at the bottom. The 1792 is the total out of 2254 reports that had enough data to determine boundary conditions for the LTP reported. It governs the total for Low–angle, SR/SS and Tidal. The 1376 is the total under solar Kpmax and MS bondaries. Data for Solar started in 1932, hence the smaller number.

The largest number is bold and underlined in each column. This number is then expressed in percent of the total. The largest percent of overlap, 16%, was that between tidal ≤± 0.10 P/A vs. ≤± 2.0d FM plus the BSF limit of ≤± 3.5-4.5 FM (four cases). The next highest, 14%, had two cases of percentages; ≤± 2.0d SR/SS vs. ≤± 0.10 P/A and solar of ≥Kpmax 6- plus ≤± 0.5d ms mag.tail vs. low–angle ≤± 2.0d SR/SS. The least percentage (5%) was for solar ≥Kpmax 6- plus ≤± 0.5d ms vs. mag.tail ≤±2.0d FM plus ≤± 3.5-4.5d FM. Thus, there were substantial percentages of overlaps between two boundary conditions. Tidal alone overlapped all other hypotheses 41% of the time. Summing up the total percentages in each column shows that the total of all percentages is 68% for all overlaps.

[Table 6]

Table 6 (Numbers and Percents of Features in Categories) Reading across the categories, Column 1 gives the number of observations (events) for each feature in each category and Column 2 gives two percentages of those numbers in Column 1. The upper percentage in Column 2 represents the percentage of the events in the category to the total events for the feature given at the bottom of the No. column. The lower percentage in Column 2 represents the percentage of that feature found in the category. The total number of events for each category is found in the right hand column. The highest number of events in each feature is bold and underlined. The category with the highest percentage in the feature is bold and underlined (upper %). The feature making up the highest percentage of a category is bold underlined and italicized (lower %).

The results of these show that in the underlined bold numbers Gaseous has 2 features, Brightenings has 6, Darkenings has none, Reddish has 3 and Bluish has none. Thus Brightenings has the most numbers of observations.

In the lower percents column, it is found that one feature, Aristarchus, had provided the highest percents in all categories. The highest percentage of each category's events was found in Aristarchus.

Figure 3 shows the percentages for each feature across each category (from Table 6) with totals at the right. The solid graphs are for the numbers in the upper row in %. The dashed graphs are for the lower row whose percentages are of the totals at the bottom for each category.

A glance at the solid–lined graphs shows that behaviors differ some but 8 out of 11 have rises at Brightenings though not the highest ones in two cases (Gassendi and Alphonsus). Two have dips there and one (Theophilus) has a low level, but not lowest, there.

Looking at the dashed graphs the results are quite mixed, many features have lows in Darkenings, (except Proclus which has its highest there). The solid and dashed graphs cannot be compared to each other.

Comparing bracketed features in the solid graph the first four behave similarly in the first three categories and differ in the other two. In the second bracket the three differ with each other. In the dashed graphs, the first group, Piton and Tycho behave somewhat similarly (both are bright features), but Alphonsus and Plato differ from them somewhat and a lot from each other (both are dark floored). In the second group all three differ considerably.

XIV. CONCLUSIONS

From these analyses found in tables and graphs for the data for all observations divided into sections designated 'All' (all observations, regardless of weight or value), '+'

(those observations in All that were confirmed or permanently recorded), '*' (those observations considered the best by not having any external influences considered in this paper), and '*+' (the * data that were confirmed or permanently recorded), the following conclusions were drawn. The data were divided into categories and into the twelve most frequently reported features, (two are combined into one – H/SV) which contributed over 60% of all observations. The categories were Brightenings, Darkenings, Reddish, Bluish, Gaseous and Negative (ones that were reported as normal – negative). The twelve features were, in order of increasing longitude from east to west IAU (aeronautical), Proclus, Theophilus, Piton, Alphonsus, Plato, Tycho, Copernicus, Gassendi, Aristarchus, Herodotus combined with Schroeter's Valley, and Grimaldi. Both categories and features were analyzed each against four hypotheses. The hypotheses were tidal, low–angle illumination, magnetic tail components and solar (particle arrivals). The tables were arranged in observations for each lunar day of age: tidal anomalistic phase, numbers of observations within specified boundary conditions, ratios of observed to expected (if no external influences acted, thus evenly distributed throughout each period), overlaps of boundary conditions and features vs. categories. In addition bias toward the terminator was assessed (but not tabulated or graphed). Tables 1a, 1b, 2a, 2b and 6 had accompanying graphs to show trends in the tables. It was found that there were differences in the behaviors of the data among both categories and features These could be readily picked out among the highest numbers and percents which were bold and underlined, but the figures showed these better. In the data for age in the categories (Table 1a) many were found to have high numbers and peaks in the magnetic tail, mostly in the magnetopause (bracketed at the left edge of Table 1a). In the figures just All (Col. 1) and *+ (Col. 4) were depicted. Negative was pretty much opposite to the positives, thus supporting the correlations. The *+ data mostly had the same trends as their All data. Some had peaks at the entrance bow–shock front (BSF) but none of the positive ones at BSF exit.

Features in the same treatment (Table 1b) also showed variations among themselves, even among those close in longitude (where the effects should be felt similarly) although the two closest ones, one degree apart, were mostly similar. The largest peaks were at sunrise (SR) for nearly all features, except Proclus, Tycho and Grimaldi. Only two (Copernicus and Gassendi) were at the BSF entrance and one at the BSF exit (Grimaldi). Several had peaks or rises within the MP. Thus two hypotheses were dominant, low–angle illumination and magnetic tail. The data depicted on the graphs in figure 1b were for All and **+**. In general the **+** data followed the All data trends.

When the data are analyzed vs. the tidal anomalistic phase (Tables 2a & 2b), there is a strong correlation with perigee (P) but lows were at apogee (A). There should be two equal ones in the hypothesis, but the lunar data do not show that.

There are many instances of rises or peaks at 0.75 Φ_d where, in theory, there should be minima. There also should be one at 0.25 Φ_d which all but Darkenings and Negative are high there. The Negative observations are somewhat opposite in behavior, seen best in the figure for these data. In view of the departures from expected behavior and despite the strong correlation at P, the correlation of categories with tidal effects is dubious. The same can be said for features vs. tidal phase. Half have peaks (not always the highest) near P, and only two have rises at or near A. Thus there is less correlation with tidal effects, even at P, among the features and only one, H/SV shows minima at 0.25 Φ_d and 0.75 Φ_d where expected.

When the data are considered, for both categories and features vs. the boundary conditions for the four hypotheses, (Tables 3a, 3b, 4a and 4b respectively) two of the latter dominate in both categories and features. These are tidal, and low–angle illumination.

The highest numbers of observations among the categories are at the largest boundary condition, at P and A combined in which five of the seven (includes Negative) with at least one division are there. There are a like number that have at least one division at low–angle illumination's largest boundary of SR/SS. There are two with one division in the magnetic tail, one in MP, the other in the BSF (Negative). Thus the data are about equally divided between tidal and low–angle illumination. None were found under solar. Expected tidal percent is 40%, which accounts for the results in ratios.

The above analyses considered just the numbers of observations and their highs. Now the data are considered as to observed numbers (and percents) vs. expected ones if there were no external influences, thus evenly distributed under the periods. This would be ratios with respect to the various boundary conditions, and would give a more accurate picture as to real correlations. Tables 4a and 4b give these results for categories and features respectively. They show considerable differences between the highest numbers and the ratios! The numbers show results as discussed above, but the ratios differ from these considerably and completely. The tidal effects are almost non–existent, all being close to unity (observed as expected), for both categories and features. Low–angle illumination is the dominant, especially at SR. There may be a bias against SS because most observing times for this condition are at early morning, an inconvenient time for those working. The low–angle ratios, vary from ~3X to > 6 times for Gaseous expected (8X for Negative + BSF). This gives a strong indication that near terminator conditions favor the detection of abnormalities in lunar aspects, implying a medium is involved therefore seen better through the longer path of light. These results favor the hypotheses of Blizard, and Sidran. It suggests that UV stimulates surface materials to luminesce, or fluoresce.

One must speculate why only ~200 out of >30,000 lunar features exhibiting similar physical properties are found to be anomalous, and only ~2200 over 1.5 millennia (averaging about 1.5/year)! The anomalies occur at all phases, not just the same one as they are found at every age of a lunation (0-29.5d).

The test for bias for terminator observances showed high numbers near it, but more than half of all observations were found over all other ages or phases of lunation. Similar phenomena in the same features were seen at other phases also.

The data were examined for overlaps of boundary conditions, which would make the correlation ambiguous and indeterminable. The highest numbers and their percents were highlighted through bold and underlining. The highest percentage of overlaps was 16% and was at the P/A of the tidal vs. the combined boundaries of the magnetic tail (MP and BSF). The lowest percentage was for solar vs. magnetic tail in their largest boundary conditions. When the percentages are added up it is found that 68% of all observations had at least two boundary conditions overlap, thus rendering them ambiguous as to which effect was operating or that two, at least were. In a few cases all hypothetical boundaries overlapped in those reported phenomena. This throws suspicion or doubt that such external influences are really affecting the Moon.

The analyses of LTP undertaken in this paper show conflicting behaviors among the data divided into the five categories, plus the negative (normal aspects) reported, and the dozen most frequently reported features. These do not show convincingly that external influences such as the hypotheses suggest are really affecting the Moon's surface. The highest correlation in ratios that really show correlations best is for terminator conditions. The various phenomena there imply a medium is involved and must be in the form of gas or dust seen through the long path of light. That there are such conditions is proved by the observations from the American landed spacecraft and the Russian ones that both observed material above the surface of the Moon, meters for Surveyor and a kilometer for the Lunakhods. The phenomena reported visually throughout the years, have been permanently recorded in various wavelengths on instruments in space and on Earth. These support the verity of phenomena occurring on the Moon that are not explainable by terrestrial atmospheric or instrumental effects. This is coupled with only ~200 features out of >30,000 seen in telescopes have ever been reported over 1500 years. Their distribution is non–random on the Moon's surface. The Apollo missions detected radon and polonium deposits. Astronauts saw some LTP while orbiting the Moon. Instruments on Earth have detected the lunar atmosphere. Finally, since some of the observations described activity that could only be attributed to a medium on the Moon, it seems inescapable that the Moon is not yet a dead world, but can and does emit materials from its interior. Judging from results in this paper it is concluded that the Moon acts independently as does the Earth. One possible use of the author's published catalog and the extension (not published yet) would be to examine the features (probably those with large numbers of reports) for a relation to the Metonic cycle of 19 years, specifically 235 months, when the features would be under the same viewing conditions. This is similar to the Saros cycle where viewing conditions on Earth for solar eclipses are the same. It would be interesting whether the same phenomena for each feature would be the same.

Appendix:

The 100 Features with >1 Reports of LTP – Locations on Plate I

Agrippa	Eimmart	Madler	Plinius
Alfraganus	Erastothenes	Maginus	Posidonius
Albategnius	Eudoxus	Manilius	Prinz
Alpetragius	Fra Mauro	Mare Vaporum	Proclus
Alphonsus	Fracastorius	Maskelyne	Ptolemaeus
Archimedes	Furneius	McClure	Pytheas
Aristarchus	Gassendi	Menelaus	Reiner
Aristillus	Godin	Mersenius	Riccioli
Atlas	Goldschmidt	Messier	Rocca
Barker's Quad	Grimaldi	Messier A	Ross
Bullialdus	Heraclides pt.	Moltke	Ross D
Calippus	Herodotus	Mt. Agassi	Ross D, SE of
Cape Agarum	Herschel, near	Mt. Hadley	Schickard
Cassini	Humboldt, West	Limb, North	Taruntius
Censorinus	Hyginus N.	Limb, South	Teneriffe Mts
Clavius	Hyginus Rill	Limb, West	Thaetetus
Cleomedes	Kepler	Peirce	Theophilus
Cobra Head (Sch Vly)	La Hire	Peirce A	Timocharis
Copernicus	LaPlace pt.	Picard	Triesnecker
Cusps, N	Leibnitz Mtns.	Picard, E. of	Tycho
Cusps, S	Lichtenburg	Pico	Vieta
Cyrillus	Linne	Pico B	Vitello
Daniell	Littrow	Pitatus	Wargentin
Dionysius	M. Crisium (N)	Piton	Webb, East of
Doerfel Mtns	Macrobius	Plato	Webb's Spot

Acknowledgements:

I acknowledge, with much gratitude to Jerry Stuart for his considerable work of suggestions, corrections and computerizing effort expended to render my manuscript, tables and graphs in computer form to conform to the modern requirements for publication in this journal.

Winifred Sawtell Cameron

Sedona, Arizona

November 2003

REFERENCES

Alter, D. 1979 In *Pictorial Guide to the Moon* pp 146-147. Thomas Y. Crowell Co., New York. NY.

Bartels, J. 1962 Geomagnetic Planetary Indices Kp, Ap, and Cp, *IAGA Bull.* **18**, 1932-1961.

Bartlett, J.C. 1967. Aristarchus, the Violet Glare. *J. Assoc. Lunar and Plan. Obs.: Strolling Astronomer* **20 (1-2),** 20-28.

Blizard. J.B. 1968. A survey of lunar transient events. *Rep. Denver Res. Inst., U of D., CO.* 575-577

Burley, J.M. and Middlehurst, B. 1966. Apparent lunar activity: historical review. *Proc. Natl. Acad. Sci.* **55**, 1007

Cameron, A.G.W. 1964. Particle acceleration in cis-lunar space. *Nature (London)* **202**, 785.

Cameron, W.S. 1972. Comparative Analyses of Observations of Lunar Transient Phenomena. *Icarus* **16,** 339-387.

Cameron, W.S. 1977. Lunar transient phenomena (LTP). Manifestations, site location, distribution, correlations and possible causes. *Phys. Earth and Planets Interiors* **14**, 194-216.

Cameron, W.S. 1978. Lunar transient phenomena (LTP) catalog. *NSSDC* **78-03**.

Cameron, W.S. 1980. New results from old data; lunar photometric anomalies in Wiley and Pohn's 1962 observations. *Astron. J.* **85,** 312-328.

Cameron, W.S. and Gilheany, J. J. 1966. Operation Moon blink and report of observations of lunar transient phenomena. *Icarus* **7 ,** 29-41.

Chapman, W.B. 1967. Tidal influences at the lunar crater Aristarchus. *J. Geophys. Res.* **72,** 6293-6298.

Elger, T.G.E. 1895. *The Moon,* Philip and Son, London, Eng. 32.

Fitton, L.E. 1975. *J. Brit. Astron. Assoc.* **65 (6) (Oct),** 519-527.

Goodacre, W. 1895. *The Moon,* Pardy and Son, Burnmouth. Eng. 37.

Graham, F. 1995. F. Graham discovers aluminum vapor in the Moon's tenuous atmosphere. *Selenology* **14 (4),** 5.

Graham, F. 1998. The atmosphere of the Moon. *Selenology* **17 (1/2)**, 41.

Green. J. 1964. Geological problems effects intensifying lunar defluidization and volcanism. *Amer. N.Y. Acad. Sci.* **123**, 403-470.

Greenacre, J.A. and Barr, E. 1963. A recent observation of lunar color phenomena. *Sky andTelescope* **26,** 316.

Harrison, D. 1970. *J. Assoc. Lun. And Planet Obs.: Strolling Astronomer* **23, (9-10)** 160-161.

Herschel, W. 1787. *Phil. Trans. Roy. Soc. London* **77,** 229-232.

Kopal, Z. 1966. Luminescence of the Moon and Solar Activity. In *Nature of the Lunar Surface* (W.N. Hess, D.H. Menzel and J.A. O'Keefe, Eds.) pp 173-184. Johns Hopkins Press, Baltimore MD.

Kopal, Z. and Rackham, T.H.. 1964. *Sky and Telescope* **21,** 140.

Kozyrev, N. 1959. Observations of a volcanic process on the Moon. *Sky and Telescope* **18,** 180.

Kozyrev, N. 1960 . In *The Moon* (Kopal, Z., Ed.) pp 96-103. Academic Press, New York

Kozyrev, N. 1962. Physical observations of the lunar surface. In *Physics and Astronomy of the Moon* (Z. Kopal , Ed.) pp 361-385.

Kozyrev, N. 1963. Volcanic phenomena on the Moon. *Nature* **198 (4884),** 979-980.

Kozyrev, N. 1964. *ACIC Technical Papers* **12,** 9

Lincoln, J.V. 1965 . Selected geomagnetic and solar data. *J. Geophys. Res.* **70**

Mattingly, T.K. 1972. Crew observations. *NASA Sp-315,* **5**, 41-43.

Middlehurst, B.M. and Moore, P .A. 1968. Lunar transient Phenomena: topographical distribution. *Science* **155 (3761),** 449 1967 (27 Jan.)

Nakamura, Y. 1976. *Proc. Lunar Sci. Conf. NASA Johnson Space Ctr.,* March, 1976, Houston, TX.

Schmitt, H.A. 1973. *NASA Sp-330*, pp 28-32

Schmitt, H.A. 1997. *Phys. Earth Planet. Int.* **14,** 217-223

Sidran, M. 1968. Thermoluminescence of the Moon. *J. Geophys. Res.* **73,** 5195-5206.

Speiser, T.W. 1967. Particle trajectories in model current sheets. 2. Analytical and numerical applications to aurorae using a geomagnetic tail model. *J. Geophys. Res.* **72,** 3919-3932.

Sprague, A.L., Hunten, D.L., Koslowski, R.W.H., Grosse, F.A., Hill, R.E. and Morris. R.L. 1998. Observations of sodium in the lunar atmosphere during international lunar atmosphere week. *Icarus* **131,** 372-381.

Wildey, R.L. and Pohn, N.A. 1964. Detailed photoelectric photometry of the Moon. *Astron. J,* **69,** 619-634.

Table 1a

NUMBERS of OBSERVATIONS for CATEGORIES vs. LUNAR AGE

	Categories: Lunar Age (Days)	LT CRV	ALL				BRIGHTENINGS				DARKENINGS				REDDISH				BLUEISH				GASEOUS				NEG	
			All	+	*	* +	All	+	*	* +	All	+	*	* +	All	+	*	* +	All	+	*	* +	All	+	*	* +	All	+
	NM 0.0 - 0.9	1	15	5	5	4	13	4	4	3	1	0	0	0	0	0	0	0	0	0	0	0	2	1	2	1	2	0
	1.0 - 1.9	5	5	2	1	1	4	1	1	1	1	1	1	1	0	0	0	0	1	1	0	0	3	1	0	0	3	0
	2.0 - 2.9	10	71	17	4	2	58	18	3	2	1	1	0	0	15	2	2	0	10	0	0	0	18	6	3	1	39	1
	3.0 - 3.9	18	141	**52**	13	7	**126**	41	10	6	11	3	0	0	33	8	1	1	41	12	2	1	53	16	8	3	53	4
	4.0 - 4.9	27	106	31	8	6	80	28	6	6	11	4	2	2	22	9	5	5	26	7	1	1	39	18	5	5	48	5
	5.0 - 5.9	37	99	40	20	12	88	**43**	11	8	23	13	2	2	38	15	8	2	30	18	8	3	58	23	17	11	39	4
	6.0 - 6.9	47	101	33	18	5	76	21	10	4	17	7	1	1	52	15	12	5	19	10	1	0	48	15	9	5	19	0
	FQ 7.0 - 7.9	58	132	38	37	12	78	23	12	2	37	11	5	2	40	10	14	7	28	20	2	2	58	23	24	8	62	0
	8.0 - 8.9	69	144	32	24	7	81	28	9	3	**48**	**19**	3	2	49	25	12	4	24	9	1	0	58	10	16	2	73	0
	9.0 - 9.9	78	110	20	19	5	59	10	6	2	38	4	3	1	44	11	11	4	15	4	0	0	43	5	13	3	56	0
BSF	10.0 - 10.9	86	103	30	31	15	50	18	8	4	34	5	2	0	37	14	15	6	12	7	3	2	**60**	21	26	14	**125**	**26**
	11.0 - 11.9	93	136	38	**43**	**20**	63	19	9	4	29	8	4	2	**67**	**33**	**24**	**13**	30	16	5	5	55	25	**27**	**15**	65	6
	12.0 - 12.9	97	127	45	30	**20**	56	24	**20**	**15**	30	16	**9**	**8**	65	31	15	10	52	**24**	**14**	**11**	53	**27**	18	12	38	4
MP	13.0 - 13.9	100	137	36	24	15	58	28	12	9	22	6	2	1	58	18	9	7	51	18	7	4	54	18	12	7	37	0
	FM 14.0 - 14.9	100	144	43	21	12	87	27	10	7	40	8	3	1	32	13	10	7	28	7	5	4	55	10	9	5	27	1
	15.0 - 15.9	97	**161**	50	23	8	95	38	10	5	31	14	2	2	48	23	5	4	**53**	13	12	2	55	16	12	0	20	0
	16.0 - 16.9	93	100	25	21	12	52	17	13	11	21	3	3	0	30	14	9	6	49	16	9	6	31	5	6	2	36	0
	17.0 - 17.9	86	100	39	27	15	62	28	17	11	22	15	6	4	31	11	7	3	41	23	11	9	38	18	14	7	25	0
BSF	18.0 - 18.9	78	67	14	11	5	24	9	1	1	17	6	1	0	24	12	9	7	22	5	4	1	14	2	5	1	30	0
	19.0 - 19.9	69	47	9	14	5	18	5	4	3	6	0	1	0	22	6	7	2	20	6	5	2	15	1	8	1	11	0
	20.0 - 20.9	58	34	3	4	3	13	1	0	0	6	0	0	0	11	3	2	2	14	1	1	0	13	3	4	3	55	0
	21.0 - 21.9	47	34	9	11	6	14	4	5	3	7	1	2	1	11	5	7	5	12	1	1	1	10	5	6	4	34	0
	LQ 22.0 - 22.9	37	29	10	9	7	14	2	2	0	4	0	0	0	8	3	3	3	5	1	1	1	15	6	6	5	18	2
	23.0 - 23.9	27	35	8	10	7	22	4	2	2	3	1	0	0	11	5	3	3	6	1	1	0	18	6	5	3	31	0
	24.0 - 24.9	18	25	2	7	2	11	1	2	1	5	0	3	0	3	1	3	1	6	1	1	1	7	1	2	1	17	0
	25.0 - 25.9	10	19	5	7	4	13	5	6	4	3	0	1	0	6	3	3	3	2	0	0	0	7	3	4	3	42	4
	26.0 - 26.9	5	20	4	4	2	13	0	0	0	3	0	1	1	3	1	0	0	6	0	0	0	5	2	3	2	7	0
	27.0 - 27.9	1	5	3	1	1	4	2	1	1	0	0	0	0	0	0	0	0	0	0	0	0	0	0	0	0	5	0
	28.0 - 28.9	0	7	2	1	1	4	2	1	1	2	0	0	0	0	0	0	0	1	0	0	0	3	1	1	1	0	0
	NM 29.0 - 29.5		0	0	0	0	0	0	0	0	0	0	0	0	0	0	0	0	0	0	0	0	0	0	0	0	0	0
	TOTAL		2254	645	448	221	1336	451	195	119	473	146	57	31	760	291	196	110	604	221	95	56	888	288	265	125	1017	57

Table 1a Cameron, Numbers of Observations for Categories vs Lunar Age

Table 1b

NUMBERS of OBSERVATIONS for FEATURES vs. LUNAR AGE

		Features	Proclus		Theophilus		Piton		Alphonsus		Plato		Tycho		Copernicus		Gassendi		Aristarchus		H/SV		Grimaldi	
			47°E	16°N	26°E	11°S	2°W	39°N	4°W	13°S	9°W	51°N	11°W	42°S	20°W	10°N	40°W	16°S	47°W	23°N	48°W	23°N	65°W	5°S
		Lunar Age (Day)	All	+	All *	+ *+	All	+	All	+	All *	+ *+	All *	+ *+	All *	+ *+	All *	+ *+	All *	+ *+	All *	+ *+	All *	+ *+
	NM	0.0 - 0.9	0	0	0	0	0	0	2	1	1 1	1 1	0	0	0	0	0	0	3 2	1 1	0	0	0	0
		1.0 - 1.9	0	0	0	0	0	0	0	0	0	0	0	0	0	0	0	0	4 0	1 0	0	0	0	0
		2.0 - 2.9	0	0	0	0	0	0	0	0	1	1	0	0	2	1	2	2	29 1	12 1	1	1	0	0
		3.0 - 3.9	3	1	0	0	0	0	0	0	6 4	3 2	2	1	6	1	1	0	46 1	20 1	3	0	4 2	3 2
		4.0 - 4.9	→2	1	1	1	0	0	0	0	3	2	0	0	1	0	0	0	46 2	16 2	1	0	1	0
		5.0 - 5.9	5	0	→6 2	1 0	0	0	0	0	2 1	1 1	0	0	1	1	2	0	38 2	21 2	1	0	4 3	3 3
		6.0 - 6.9	6	1	2	0	1	0	3	1	3 1	0 0	0	0	0	0	0	0	14 0	7 0	0	0	0	0
	FQ	7.0 - 7.9	11	2	2 1	1 1	→7	2	→10	4	→1	1	→0	0	1	0	0	0	5 1	2 0	1	0	0	0
		8.0 - 8.9	10	3	1	1	3	0	9	5	24 4	3 2	3 1	0 0	2	0	0	0	6 0	2 0	0	0	1	1
		9.0 - 9.9	12	2	0	0	1	0	7	4	17 2	5 1	3	0	→9 1	0 0	2	1	5 0	1 0	0	0	0	0
BSF		10.0 - 10.9	11	1	0	0	2	0	6	5	16 4	8 4	1	1	1	0	→9 4	3 2	8 1	3 1	0	0	0	0
BSF		11.0 - 11.9	12	0	0	0	0	0	2	1	15 3	5 2	1	0	0	0	20 11	7 6	→38 10	8 7	→11 3	2 2	0	0
		12.0 - 12.9	2	0	0	0	0	0	0	0	12 3	6 3	0	0	1 1	1 1	5 1	2 1	56 12	21 8	18 2	6 2	→0	0
MP		13.0 - 13.9	5	0	0	0	2	0	2	1	14 6	6 5	2	0	0	0	2	0	49 5	16 4	11 2	4 2	2	0
MP	FM	14.0 - 14.9	10	2	0	0	0	0	1	0	8	2	6	3	2	0	0	0	49 9	17 8	10 1	1 0	2	1
MP		15.0 - 15.9	13	2	0	0	0	0	1	1	11 2	4 1	0	0	5 1	3 1	2	1	41 7	18 1	7 2	3 0	2	2
MP		16.0 - 16.9	10	2	0	0	0	0	2	1	9 3	3 2	0	0	1	0	5 1	2 1	42 6	10 3	2	0	0	0
		17.0 - 17.9	←4	0	0	0	2	0	0	0	12 2	3 2	0	0	2 1	2 1	3	1	32 6	14 6	6 1	1 0	1	0
BSF		18.0 - 18.9	3	1	2 1	1 1	0	0	2	0	8 1	3 1	0	0	0 1	0 0	0	0	19 3	3 2	3 2	0 0	3 2	0 0
BSF		19.0 - 19.9	1	0	←1 1	1 1	2	0	1	0	3	0	0	0	1 1	0 0	1	0	18 4	4 2	1	0	0	0
		20.0 - 20.9	0	0	0	0	0	0	1	1	0	0	0	0	1	0	1 1	1 1	14 1	1 1	1	0	0	0
		21.0 - 21.9	0	0	0	0	0	0	2	1	1	0	0	0	1	0	1 1	0 0	16 2	4 2	0	0	0	0
	LQ	22.0 - 22.9	0	0	0	0	←0	0	←3	2	←2 2	0 0	2	2	4	1	1	0	9 1	1 1	2 1	1 1	0	0
		23.0 - 23.9	0	0	0	0	0	0	0	0	5 1	1 0	←3	0	←1	1	0	0	12 4	3 3	0	0	1 1	1 1
		24.0 - 24.9	0	0	0	0	0	0	0	0	0	0	0	0	1	0	←0	0	7 3	1 1	0	0	1 1	0 0
		25.0 - 25.9	0	0	0	0	0	0	0	0	0	0	0	0	0	0	0	0	←7 2	2 1	←4 3	3 3	0	0
		26.0 - 26.9	0	0	0	0	0	0	1	1	2	1	0	0	0	0	0	0	1 0	0 0	0	0	←4 2	0 0
		27.0 - 27.9	1	0	0	0	0	0	1	1	0	0	0	0	0	0	0	0	0 0	0 0	0	0	0	0
		28.0 - 28.9	0	0	0	0	0	0	0	0	0	0	0	0	1	1	0	0	2 1	1 1	0	0	0	0
	NM	29.0 - 29.5	0	0	0	0	0	0	0	0	0	0	0	0	0	0	0	0	0	0	0	0	0	0
		TOTAL	121	18	15 5	6 3	20	2	56	30	176 40	59 27	23 1	7 0	44 6	12 3	57 19	20 11	616 86	210 59	63 17	22 10	26 11	11 6

Table 1b Cameron, Numbers of Observations for Features vs Lunar Age

Table 2a

NUMBERS OF OBSERVATIONS for CATEGORIES vs. TIDAL ANOMALSTIC PHASE (φd)

Anomalistic Phase (φd)	ALL				BRIGHTENINGS				DARKENINGS				REDDISH				BLUISH				GASEOUS				NEGATIVE		MIDDLEHURST
Boundaries	All	+	*	* +	All	+	*	* +	All	+	*	* +	All	+	*	* +	All	+	*	* +	All	+	*	* +	All	+	All
P 0.950-0.049	**298**	**101**	58	**39**	**206**	**75**	**33**	**26**	49	15	6	4	91	**42**	24	18	86	36	**20**	**15**	107	**41**	33	17	90	0	**27**
0.050-0.149	222	56	40	17	151	51	21	13	37	4	4	1	74	23	17	8	53	16	10	7	90	18	21	8	116	**10**	17
0.150-0.249	225	57	36	16	155	47	18	7	47	18	4	2	91	31	18	4	62	21	1	0	83	31	23	9	108	2	15
0.250-0.349	177	37	36	14	83	20	12	6	46	10	**8**	3	61	21	18	9	29	6	3	1	76	23	25	9	**131**	3	6
0.350-0.449	227	52	47	20	136	31	20	10	**54**	10	7	2	**94**	26	13	6	45	12	7	1	**108**	31	29	15	77	1	3
A 0.450-0.549	168	47	33	11	86	30	11	6	49	22	7	**5**	50	15	10	5	43	11	8	1	70	13	18	3	65	5	23
0.550-0.649	198	65	32	16	95	37	10	9	42	17	6	3	62	31	15	9	**87**	**43**	8	4	79	36	19	9	77	1	7
0.650-0.749	223	72	**59**	32	146	67	23	12	46	16	7	3	81	**42**	**36**	**22**	66	23	14	9	102	38	31	11	77	8	11
0.750-0.849	217	51	41	20	114	32	14	7	43	7	4	2	78	28	18	12	60	27	10	8	63	20	21	13	127	0	18
0.850-0.949	237	69	53	31	113	41	23	16	49	**23**	4	3	72	33	22	17	63	23	9	7	100	33	**36**	**22**	124	2	18
Totals	2192	607	435	216	1285	431	185	112	462	142	57	28	754	282	191	110	594	218	90	53	878	284	256	116	992	32	145

Table 2a Cameron, Numbers of Observations for Categories vs Tidal Anomalistic Phase

Table 2b

NUMBERS of OBSERVATIONS for FEATURES vs. TIDAL ANOMALISTIC PHASE (φ_d)

Features	Proclus		Theophilus		Piton		Alphonsus		Plato		Tycho		Copernicus		Gassendi		Aristarchus		H/SV		Grimaldi	
	47°E	16°N	26°E	11°S	2°W	39°N	4°W	13°S	9°W	51°N	11°W	42°S	20°W	10°N	40°W	16°S	47°W	23°N	48°W	23°N	65°W	5°S
Anomalistic	All	+	All	+	All	+	All	+	All	+	All	+	All	+	All	+	All	+	All	+	All	+
Phase (φd)	*	* +	*	* +	*	* +	*	* +	*	* +	*	* +	*	* +	*	* +	*	* +	*	* +	*	* +
P 0.950-0.049	23	2	0	0	2	0	5	2	19	7	3	1	3	2	11	4	96	40	15	4	5	2
	0	0	0	0	1	0	2	2	5	4	0	0	0	0	2	2	15	11	1	0	0	0
0.050-0.149	23	5	1	1	1	0	6	4	11	1	2	1	4	0	4	1	60	20	5	0	1	1
	0	0	0	0	0	0	4	3	1	0	0	0	0	0	2	0	6	3	0	0	1	1
0.150-0.249	8	1	3	0	4	0	2	1	11	3	3	0	4	1	4	0	61	20	6	1	2	0
	0	0	1	0	3	0	1	0	3	2	0	0	0	0	1	0	3	2	1	0	0	0
0.250-0.349	12	1	3	1	6	0	6	4	14	4	1	0	6	3	6	4	29	7	5	1	1	0
	0	0	2	0	5	0	3	2	3	2	0	0	0	0	4	3	2	1	1	1	0	0
0.350-0.449	4	0	2	0	2	0	8	4	23	10	3	0	4	0	2	0	58	18	15	3	1	0
	0	0	0	0	2	0	3	0	6	4	0	0	0	0	0	0	13	7	4	2	0	0
A 0.450-0.549	8	1	1	1	3	0	1	1	14	7	2	0	1	0	7	2	54	15	11	3	2	0
	2	1	0	0	0	0	0	0	2	2	0	0	0	0	2	1	6	3	4	2	0	0
0.550-0.649	7	2	2	1	0	0	3	2	19	6	1	0	4	1	3	2	68	26	8	1	4	1
	0	0	1	1	0	0	3	2	6	4	0	0	0	0	1	1	5	4	0	0	0	0
0.650-0.749	9	2	2	1	4	1	4	2	12	3	0	0	2	0	2	1	73	26	1	0	7	1
	0	0	0	0	3	1	2	1	3	1	0	0	1	0	1	1	10	8	0	0	0	0
0.750-0.849	10	1	1	1	0	0	15	5	25	7	4	2	7	1	6	3	50	12	2	1	1	0
	0	0	1	1	0	0	7	3	4	1	0	0	0	0	3	2	9	7	1	1	0	0
0.850-0.949	14	3	0	0	2	1	6	5	19	4	4	3	6	2	11	1	60	24	15	6	4	0
	0	0	0	0	1	1	2	1	4	1	0	0	2	1	3	0	15	12	4	4	0	0
Totals	118	18	15	6	24	2	56	30	167	52	23	7	41	10	56	18	609	208	83	20	28	5
	2	1	5	2	15	2	27	14	27	22	0	0	3	1	19	10	84	58	16	10	1	1

Table 2b Cameron, Numbers of Observations for Features vs Tidal Anomalistic Phase (φ_d)

Table 3a

Numbers of Observations for Categories in Boundaries of Hypotheses

Categories	All				Gaseous				Darkenings				Brightenings				Reddish				Bluish				Negative	
Boundaries	All	+	*	* +	All	+	*	* +	All	+	*	* +	All	+	*	* +	All	+	*	* +	All	+	*	* +	All	+
Tidal																										
≤± 0.100 P	501	133	94	61	198	61	51	28	92	30	11	7	201	100	47	37	153	70	40	26	147	56	26	17	182	2
≤± 0.100 A	367	104	77	32	131	36	42	15	100	36	14	7	176	57	24	17	129	49	23	11	109	50	14	4	150	6
≤± 0.100 P/A	**868**	**237**	171	93	**329**	97	93	43	**192**	**66**	**25**	**14**	**377**	157	71	**54**	282	119	63	37	**256**	**106**	**40**	**21**	332	8
Totals	2192	607	435	216	878	284	256	116	462	142	57	28	1285	431	185	119	754	292	190	108	594	220	90	53	992	32
Low-Angle Illumination																										
≤+ 2.0d SR	444	120	160	71	267	88	99	58	117	43	13	8	284	83	53	28	237	86	78	38	137	52	16	10	270	15
≤− 2.0d SS	115	29	43	25	55	20	28	18	27	7	6	1	80	23	26	14	53	37	19	14	27	9	4	2	107	5
≤± 2.0d SR/SS	559	149	**203**	**96**	322	**108**	**127**	**76**	144	50	19	9	364	106	**79**	42	**290**	**123**	**97**	**52**	164	61	20	12	**377**	20
Totals	2296	687	448	221	888	288	265	125	473	148	57	29	1294	430	195	119	742	286	196	124	598	221	91	51	961	58
Magnetic Tail																										
≤± 2.0d FM MP	529	145	102	56	208	53	46	17	112	36	13	7	303	**175**	52	38	178	50	28	20	150	58	35	17	111	2
≤± 3.5d-4.5d FM BSF	176	41	40	2	66	19	22	9	48	12	4	0	81	47	9	3	61	17	33	11	11	43	13	5	138	**33**
Totals	2283	676	448	221	888	288	265	125	473	148	57	25	1336	450	195	119	758	298	196	124	604	221	91	53	1017	58
Solar																										
≥Kp max 6−	158	40	23	14	55	18	17	9	33	6	4	2	93	27	13	7	52	21	11	7	63	26	11	10	112	4
≤± 0.50 MS	392	113	72	36	114	36	34	14	74	15	14	5	213	68	28	16	121	72	39	29	89	33	16	10	182	4
Totals	1905	612	381	187	724	263	208	113	451	131	48	23	1070	131	48	23	679	265	163	94	540	198	89	53	905	58

Table 3a Cameron, Numbers of Observations for Categories in Boundaries of Hypotheses

Table 3b

Numbers of Observations for Features in Boundaries of Hypotheses

Features	Proclus 47°E 16°N		Theophilus 26°E 11°S		Piton 2°W 39°N		• Alphonsus 4°W 13°S		• Plato 9°W 51°N		Tycho 11°W 42°S		Copernicus 20°W 10°N		• Gassendi 40°W 16°S		Aristarchus 47°W 23°N		• H/SV 48°W 23°N		• Grimaldi 65°W 5°S	
Boundaries	All *	+ *+	All *	+ *+	All *	+ *+	All *	+ *+	All *	+ *+	All *	+ *+	All *	+ *+	All *	+ *+	All *	+ *+	All *	+ *+	All *	+ *+
Tidal																						
≤± 0.100 P	47	9	0	0	2	0	9	5	40	16	5	2	8	2	18	7	160	61	28	5	4	1
	0	0	0	0	0	0	3	3	8	6	0	0	2	**2**	3	2	28	19	2	0	0	0
≤± 0.100 A	14	2	5	2	2	0	8	4	37	10	4	0	7	1	11	5	122	39	23	6	3	1
	0	0	0	0	0	0	4	2	6	4	0	0	0	0	3	2	15	10	4	2	0	0
≤± 0.100 P/A	**61**	**11**	5	2	4	0	17	9	**77**	**26**	9	2	15	3	29	**12**	**282**	**100**	**51**	11	7	2
	0	0	0	0	0	0	7	5	**14**	**10**	0	0	**2**	**2**	6	4	**43**	**29**	6	2	0	0
Totals	118	18	15	6	24	2	56	30	172	56	17	6	41	10	56	18	609	208	83	20	27	7
	0	0	0	0	15	2	27	14	42	19	0	0	2	2	19	10	84	58	16	10	9	4
Low-Angle Illumination																						
≤+ 2.0d SR	9	2	8	2	11	**2**	28	13	48	13	5	0	12	0	**30**	9	115	40	37	11	5	1
	0	0	2	0	8	**2**	15	8	8	5	0	0	2	0	**14**	5	26	18	7	6	2	0
≤– 2.0d SS	12	2	2	2	1	0	6	4	6	1	5	1	7	2	0	0	16	4	5	3	5	0
	0	0	2	2	1	0	4	4	2	0	0	0	0	0	0	0	6	2	3	3	1	0
≤± 2.0d SR/SS	21	4	**10**	**4**	**12**	**2**	**34**	**17**	54	14	**10**	1	**19**	2	**30**	9	131	44	42	**14**	**10**	1
	0	0	**4**	**2**	**9**	**2**	**19**	**12**	10	5	0	0	**12**	0	**14**	**5**	32	20	**10**	**9**	**3**	0
Totals	121	18	15	6	24	2	56	30	176	59	23	7	42	12	57	20	614	209	85	22	27	11
	0	0	5	3	15	2	27	14	39	26	0	0	16	2	19	11	85	58	17	10	11	6
Magnetic Tail																						
≤± 2.0d FM MP	39	6	0	0	4	0	4	1	43	13	9	**3**	10	**5**	8	2	191	64	37	7	7	**4**
	0	0	0	0	2	0	1	0	6	6	0	0	0	0	0	0	30	18	4	1	1	**1**
≤± 3.5d-4.5d FM BSF	12	1	5	2	3	0	9	5	21	5	1	1	1	0	17	6	40	9	4	0	0	0
	0	0	0	0	2	0	3	0	3	1	0	0	0	0	8	2	5	3	2	0	0	0
Totals	121	18	15	6	24	4	56	30	176	59	23	7	44	12	57	18	616	209	83	20	27	12
	0	0	5	3	4	4	27	14	39	26	0	0	3	3	19	11	86	59	17	10	11	6
Solar																						
≥Kp max 6-	5	0	1	1	2	0	4	3	18	4	2	0	5	1	3	2	46	15	4	0	0	0
	0	0	0	0	1	0	2	2	3	3	0	0	1	1	0	0	7	6	1	0	0	0
≤± 0.50d MS	20	2	3	2	5	0	10	8	27	8	5	1	9	3	6	5	95	32	8	1	2	1
	0	0	2	1	3	0	5	4	6	4	0	0	0	0	2	2	14	10	2	0	0	0
Totals	109	18	11	5	24	2	49	26	115	43	17	6	43	12	51	16	517	188	63	21	25	12
	5	2	4	4	11	2	25	13	30	21	0	0	1	1	18	9	75	53	16	10	0	0

Table 3b Cameron, Features - Numbers of Observations for Categories in Boundaries of Hypotheses

Table 4a

Categories - Ratios of Percents of Observations to Expected in Boundaries of Hypotheses

Categories	ALL				Brightenings				Darkenings			
	Obs. No.	Obs. %	Exp. %	O/E	Obs. No.	Obs. %	Exp. %	O/E	Obs. No.	Obs. %	Exp. %	O/E
Boundaries	All *+				All *+				All *+			
Tidal												
≤± 0.100 P	501 61	23 28	20	1.2 1.4	201 37	16 31	20	0.8 1.6	92 7	20 25	20	1.0 1.2
≤± 0.100 A	367 32	17 15	20	0.8 0.8	176 17	14 14	20	0.7 0.7	100 7	22 25	20	1.1 1.2
≤± 0.100 P/A	**868** 93	40 43	40	1.0 1.1	**377** **54**	29 45	40	0.7 1.1	**192** **14**	42 50	40	1.0 1.2
Totals	2192 216				1285 119				462 28			
Low-Angle Illumination												
≤+ 2.0d SR	444 71	19 32	7	***2.7*** ***4.6***	284 28	22 24	7	***3.1*** ***3.4***	117 8	25 28	7	***3.6*** ***4.0***
≤– 2.0d SS	115 25	5 11	7	0.7 1.6	80 14	6 12	7	0.9 1.7	27 1	6 3	7	0.9 0.4
≤± 2.0d SR/SS	559 **96**	24 43	14	1.7 3.1	364 42	28 35	14	2.0 2.5	144 9	30 31	14	2.1 2.2
Totals	2296 221				1294 119				473 29			
Magnetic Tail												
≤± 2.0d FM MP	529 56	23 25	14	1.6 1.8	303 38	23 32	14	1.6 2.3	112 7	24 28	14	1.7 2.0
≤± 3.5d - 4.5d FM BSF	176 2	8 1	7	1.1 0.1	81 3	6 3	7	0.9 0.4	48 0	10 0	7	1.4 0.0
Totals	2283 221				1336 119				473 25			
Solar												
≥Kp max 6–	158 14	8 7	9	0.9 0.8	93 7	9 30	9	1.0 3.4	33 2	7 9	9	0.8 1.0
≤± 0.50d MS	392 36	21 19	18	1.2 1.1	213 16	20 70	18	1.1 3.9	74 5	16 22	18	0.9 1.2
Totals	1905 187				1070 23				451 23			

Categories	Reddish				Bluish				Gaseous				Negative			
	Obs. No.	Obs. %	Exp. %	O/E	Obs. No.	Obs. %	Exp. %	O/E	Obs. No.	Obs. %	Exp. %	O/E	Obs. No.	Obs. %	Exp. %	O/E
Boundaries	All *+				All *+				All *+				All *+			
Tidal																
≤± 0.100 P	153 26	20 24	20	1.0 1.2	147 17	25 32	20	1.2 1.6	198 28	23 24	20	1.2 1.2	182 2	18 6	20	0.9 0.3
≤± 0.100 A	129 11	17 10	20	0.8 0.5	109 4	18 8	20	0.9 0.4	131 15	15 13	20	0.8 0.6	150 6	15 19	20	0.8 1.0
≤± 0.100 P/A	282 37	37 34	40	0.9 0.8	**256** **21**	43 40	40	1.1 1.0	**329** 43	37 37	40	0.9 0.9	332 8	33 25	40	0.8 0.6
Totals	754 108				594 53				878 116				992 32			
Low-Angle Illumination																
≤+ 2.0d SR	237 38	32 31	7	***4.6*** ***4.4***	137 10	23 20	7	***3.3*** ***2.9***	267 58	30 46	7	***4.3*** ***6.6***	270 15	28 26	7	***4.0*** 3.7
≤– 2.0d SS	53 14	7 11	7	1.0 1.6	27 2	5 4	7	0.7 0.6	55 18	6 14	7	0.9 2.0	107 5	11 9	7	1.6 1.3
≤± 2.0d SR/SS	**290** **52**	39 42	14	2.8 3.0	164 12	27 24	14	1.9 1.7	322 **76**	36 61	14	2.6 4.4	**377** 20	39 34	14	2.8 2.4
Totals	742 124				598 51				888 125				961 58			
Magnetic Tail																
≤± 2.0d FM MP	178 20	23 16	14	1.6 1.1	150 17	25 32	14	1.8 2.3	208 17	23 14	14	1.6 1.0	111 2	11 3	14	0.8 0.2
≤± 3.5d - 4.5d FM BSF	61 11	8 9	7	1.1 1.3	11 5	2 9	7	0.3 1.3	66 9	7 7	7	1.0 1.0	138 **33**	14 57	7	2.0 ***8.1***
Totals	758 124				604 53				888 125				1017 58			
Solar																
≥Kp max 6–	52 7	8 7	9	0.9 0.8	63 10	12 19	9	1.3 2.1	55 9	8 8	9	0.9 0.9	112 4	12 7	9	1.3 0.8
≤± 0.50d MS	121 29	18 31	18	1.0 1.7	89 10	16 19	18	0.9 1.1	114 14	16 13	18	0.9 0.7	182 4	20 7	18	1.1 0.4
Totals	679 94				540 53				724 113				905 58			

Table 4a Cameron, Categories - Ratios of percents of Observations in Boundaries of Hypotheses

Table 4b

Features - Ratios of Percents Observed to Expected in Boundaries of Hypotheses

Features	Proclus 47°E 16°N				Theophilus 26°E 11°S				Piton 2°W 39°N				● Alphonsus 4°W 13°S				● Plato 9°W 51°N			
	Obs. No.	Obs. %	Exp. %	O/E	Obs. No.	Obs. %	Exp. %	O/E	Obs. No.	Obs. %	Exp. %	O/E	Obs. No.	Obs. %	Exp. %	O/E	Obs. No.	Obs. %	Exp. %	O/E
Boundaries	All,				All,				All,				All,				All,			
	+				+				+				+				+			
Tidal																				
≤± 0.100 P	47	40	20	2.0	0	0	20	0.0	2	8	20	0.4	9	16	20	0.8	40	23	20	1.2
	9	50		**2.5**	0	0		0.0	0	0		0.0	5	17		0.8	16	29		1.4
≤± 0.100 A	14	12	20	0.6	5	33	20	1.6	2	8	20	0.4	8	14	20	0.7	37	22	20	1.1
	2	11		0.6	2	33		1.6	0	0		0.0	4	13		0.6	10	18		0.9
≤± 0.100 P/A	**61**	52	40	1.3	5	33	40	0.8	4	17	40	0.4	17	30	40	0.8	**77**	45	40	1.1
	11	61		1.5	2	33		0.8	0	0		0.0	9	30		0.8	**26**	46		1.2
Totals	118				15				24				56				172			
	18				6				15				30				56			
Low-Angle Illumination																				
≤+ 2.0d SR	9	7	7	1.0	8	53	7	**7.6**	11	46	7	**6.6**	28	50	7	**7.1**	48	27	7	**3.9**
	2	11		1.6	2	40		4.7	2	13		**1.9**	13	43		**6.1**	13	22		**3.1**
≤- 2.0d SS	12	10	7	1.4	2	13	7	1.9	1	4	7	0.6	6	11	7	1.6	6	3	7	0.4
	2	11		1.6	2	40		4.7	0	0		0.0	4	13		1.9	1	1		0.1
≤± 2.0d SR/SS	21	17	14	1.2	**10**	67	14	4.8	**12**	50	14	3.6	**34**	61	14	4.4	54	31	14	2.2
	4	22		1.6	**4**	80		**5.7**	**2**	13		1.0	**17**	57		4.1	14	24		1.7
Totals	121				15				24				56				176			
	18				5				15				30				59			
Magnetic Tail																				
≤± 2.0d FM MP	39	32	14	**2.3**	0	0	14	0.0	4	17	14	1.2	4	7	14	0.5	43	24	14	1.7
	6	33		2.4	0	0		0.0	0	0		0.0	1	3		0.2	13	22		1.6
≤± 3.5d-4.5d FM BSF	12	10	7	1.4	5	33	7	4.7	3	12	7	1.7	9	16	7	2.3	21	12	7	1.7
	1	6		0.9	2	33		4.7	0	0		0.0	5	17		2.4	5	8		1.1
Totals	121				15				24				56				176			
	18				6				4				30				59			
Solar																				
≥Kp max 6–	5	5	9	0.6	1	9	9	1.0	2	8	9	0.9	4	8	9	0.9	18	16	9	1.8
	0	0		0.0	1	20		2.2	0	0		0.0	3	12		1.3	4	9		1.0
≤± 0.50d MS	20	18	18	1.0	3	27	18	1.5	5	21	18	1.2	10	20	18	1.1	27	23	18	1.3
	2	11		0.6	2	40		2.2	0	0		0.0	8	31		1.7	8	19		1.1
Totals	109				11				24				49				115			
	18				5				2				26				43			

Features	Tycho 11°W 42°S				Copernicus 20°W 10°N				● Gassendi 40°W 16°S				Aristarchus 47°W 23°N				● H/SV 48°W 23°N			
	Obs. No.	Obs. %	Exp. %	O/E	Obs. No.	Obs. %	Exp. %	O/E	Obs. No.	Obs. %	Exp. %	O/E	Obs. No.	Obs. %	Exp. %	O/E	Obs. No.	Obs. %	Exp. %	O/E
Boundaries	All,				All,				All,				All,				All,			
	+				+				+				+				+			
Tidal																				
≤± 0.100 P	5	29	20	1.4	8	20	20	1.0	18	32	20	1.6	160	26	20	1.3	28	34	20	1.7
	2	33		1.6	2	20		1.0	7	39		2.0	61	29		1.4	5	25		1.2
≤± 0.100 A	4	24	20	1.2	7	17	20	0.8	11	20	20	1.0	122	20	20	1.0	23	28	20	1.4
	0	0		0.0	1	10		0.5	5	28		1.4	39	19		1.0	6	30		1.5
≤± 0.100 P/A	9	53	40	1.3	15	37	40	0.9	29	52	40	1.3	**282**	46	40	1.2	**51**	61	40	1.5
	2	33		0.8	3	30		0.8	**12**	67		1.7	**100**	48		1.2	11	55		1.4
Totals	17				41				56				609				83			
	6				10				18				208				20			
Low-Angle Illumination																				
≤+ 2.0d SR	5	22	7	**3.1**	12	29	7	**4.1**	**30**	53	7	**7.6**	115	19	7	**2.7**	37	44	7	**6.3**
	0	0		0.0	0	0		0.0	9	45		**6.4**	40	19		**2.7**	11	50		**7.1**
≤- 2.0d SS	5	22	7	**3.1**	7	17	7	2.4	0	0	7	0.0	16	3	7	0.4	5	6	7	0.9
	1	14		**2.0**	2	17		2.4	0	0		0.0	4	2		0.3	3	14		2.0
≤± 2.0d SR/SS	**10**	43	14	**3.1**	**19**	45	14	3.2	**30**	53	14	3.8	131	21	14	1.5	42	49	14	3.5
	1	14		1.0	2	17		1.2	9	45		3.2	44	21		1.5	**14**	64		4.6
Totals	23				42				57				614				85			
	7				12				20				209				22			
Magnetic Tail																				
≤± 2.0d FM MP	9	39	14	2.8	10	23	14	1.6	8	14	14	1.0	191	31	14	2.2	37	45	14	3.2
	3	43		**3.1**	**5**	42		**3.0**	2	11		0.8	64	31		2.2	7	35		2.5
≤± 3.5d-4.5d FM BSF	1	4	7	0.6	1	2	7	0.3	17	30	7	4.3	40	7	7	1.0	4	5	7	0.7
	1	14		2.0	0	0		0.0	6	33		4.7	9	4		0.6	0	0		0.0
Totals	23				44				57				616				83			
	7				12				18				209				20			
Solar																				
≥Kp max 6–	2	12	9	1.3	5	12	9	1.3	3	6	9	0.7	46	9	9	1.0	4	6	9	0.7
	0	0		0.0	1	8		0.9	2	12		1.3	15	8		0.9	0	0		0.0
≤± 0.50d MS	5	29	18	1.6	9	21	18	1.2	6	12	18	0.7	95	18	18	1.0	8	13	18	0.7
	1	17		0.9	3	25		1.4	5	31		1.7	32	17		0.9	1	5		0.3
Totals	17				43				51				517				63			
	6				12				16				188				21			

Features	● Grimaldi 65°W 5°S				XXX Plato 9°W 51°N				XXX Aristarchus 47°W 23°N			
	Obs. No.	Obs. %	Exp. %	O/E	Obs. No.	Obs. %	Exp. %	O/E	Obs. No.	Obs. %	Exp. %	O/E
Boundaries	All,				*				*			
	+				* +							
Tidal												
≤± 0.100 P	4	15	20	0.8	8	19	20	1.0	28	33	20	1.6
	1	14		0.7	6	32		1.6				
≤± 0.100 A	3	11	20	0.6	6	14	20	0.7	15	18	20	0.9
	1	14		0.7	4	21		1.1				
≤± 0.100 P/A	7	26	40	0.6	**14**	33	40	0.8	**43**	51	40	1.3
	2	29		0.7	**10**	53		0.8				
Totals	27				42				84			
	7				19							
Low-Angle Illumination												
≤+ 2.0d SR	5	19	7	**2.7**	8	21	7	**2.9**	26	31	7	**4.4**
	1	9		1.3	5	19		**2.7**				
≤- 2.0d SS	5	19	7	**2.7**	2	5	7	0.7	6	7	7	1.0
	0	0		0.0	0	0		0.0				
≤± 2.0d SR/SS	**10**	37	14	2.6	10	26	14	1.8	32	38	14	2.7
	1	9		0.6	5	19		1.4				
Totals	27				39				85			
	11				26							
Magnetic Tail												
≤± 2.0d FM MP	7	26	14	1.9	6	15	14	1.1	30	35	14	2.5
	4	33		**2.4**	6	23		1.6				
≤± 3.5d-4.5d FM BSF	0	0	7	0.0	3	8	7	1.1	5	6	7	0.9
	0	0		0.0	1	4		0.6				
Totals	27				39				86			
	12				26							
Solar												
≥Kp max 6–	0	0	9	0.0	3	10	9	1.1	7	9	9	1.0
	0	0		0.0	3	14		1.6				
≤± 0.50d MS	2	8	18	0.4	6	20	18	1.1	14	19	18	1.1
	1	8		0.4	4	19		1.1				
Totals	25				30				75			
	12				21							

Table 4b Cameron, Features - Ratios of Percents Observed to Expected in Boundaries of Hypotheses

Table 5

Category Overlaps of Boundary Conditions

Tidal: A		Tidal: B		Tidal: C		Magnetic Tail: D		Magnetic Tail: E		Low-angle Illumination: F	
Magnetic Tail	No.	Low-angle illumination	No.	Solar	No.	Low-angle Illumination	No.	Solar	No.	Solar	No.
≤± 2.0d FM vs. ≤± 0.100 P	163	≤+ 2.0d SR vs. ≤± 0.100 P	119	≥Kp max 6- vs. ≤± 0.100 P	32	≤+ 2.0d SR vs. ≤± 2.0d FM	54	≥Kp max 6- vs. ≤± 2.0d FM	16	≥Kp max 6- vs. ≤+ 2.0d SR	45
≤± 2.0d FM vs. ≤± 0.100 A	89	≤+ 2.0d SR vs. ≤± 0.100 A	82	≥Kp max 6- vs. ≤± 0.100 A	22	≤– 2.0d SS vs. ≤± 2.0d FM	64	≤± 0.5d ms vs. ≤± 2.0d FM	37	≥Kp max 6- vs. ≤– 2.0d SS	11
≤± 2.0d FM vs. ≤± 0.100 P/A	252	≤– 2.0d SS vs. ≤± 0.100 P	32	≤± 0.5d ms vs. ≤± 0.100 P	64	≤+ 2.0d SR vs. ≤± 3.5d-4.5d FM	16	≥Kp max 6- vs. ≤± 3.5d-4.5d FM	6	≤± 0.50d ms vs. ≤+ 2.0d SR	76
≤± 3.5d-4.5d FM vs. ≤± 0.100 P	23	≤- 2.0d SS vs. ≤± 0.100 A	21	≤± 0.5d ms vs. ≤± 0.100 A	36	≤– 2.0d SS vs. ≤± 3.5d-4.5d FM	18	≤± 0.5d ms vs. ≤± 3.5d-4.5d FM	14	≤± 0.50d ms vs. ≤– 2.0d SS	56
≤± 3.5d-4.5d FM vs. ≤± 0.100 A	20	≤± 2.0d SR/SS vs. ≤± 0.100 P	151	≥Kp max 6- vs. ≤± 0.100 P/A	54	≤± 2.0d SR/SS vs. ≤± 2.0d FM	118	≥Kp max 6- + ≤ 0.5d ms vs. ≤± 2.0d FM	53	≥Kp max 6- vs. ≤± 2.0d SR/SS	56
≤± 3.5d-4.5d FM vs. ≤± 0.100 P/A	43	≤± 2.0d SR/SS vs. ≤± 0.100 A	103	≤± 0.5d ms vs. ≤± 0.100 P/A	100	≤± 2.0d SR/SS vs. ≤± 3.5d-4.5d FM	34	≥Kp max 6- + ≤±0.5d ms vs. ≤± 3.5d-4.5d FM	20	≤± 0.50d ms vs. ≤± 2.0d SR/SS	132
≤± 2.0d FM + ≤± 3.5d-4.5d FM vs. ≤± 0.100 P/A	**295**	≤± 2.0d SR/SS vs. ≤± 0.100 P/A	**254**	≥Kp max 6- + ≤± 0.5d ms vs. ≤± 0.100 P/A	**154**	≤± 2.0d SR/SS vs. ≤± 2.0d FM + ≤± 3.5d-4.5d FM	**152**	≥Kp max 6- + ≤± 0.5d ms vs. ≤± 2.0d FM + ≤± 3.5d-4.5d FM	**73**	≥Kp max 6- + ≤± 0.5d ms vs. ≤± 2.0d SR/SS	**188**
Totals	1792		1792		1376		1792		1376		1376
Percent	***16%***		**14%**		**11%**		**8%**		**5%**		**14%**

% of Total overlaps = 68%

Table 5 Cameron, Category Overlaps of Boundary Conditions

Table 6

FEATURES vs. CATEGORIES

	Features	Proclus		Theophilus		Piton		• Alphonsus		• Plato		Tycho		Copernicus		• Gassendi		Aristarchus		• H/SV		• Grimaldi			
Category		No.	%	No.	%	No.	%	No.	%	No.	%	No.	%	No.	%	No.	%	No.	%	No.	%	No.	%	Category Totals	Category Highs
Gaseous	Category %		17		22		**40**		21		29		30		11		17		17		**36**		14		
	# of Events	28		7		**17**		18		72		13		6		13		155		**53**		5		387	2
	Feature %		7		2		4		5		19		3		2		3		**40**		14		1		
Brightenings	Category %		**35**		22		28		29		**34**		**48**		**54**		21		**38**		21		**38**		
	# of Events	**57**		7		12		25		**85**		**21**		**29**		16		**334**		31		**14**		631	6
	Feature %		9		1		2		4		13		3		5		3		**53**		5		2		
Darkenings	Category %		28		0		9		11		11		2		6		9		6		6		8		
	# of Events	45		0		4		9		28		1		3		7		57		9		3		166	0
	Feature %		27		0		2		5		17		1		2		4		**34**		5		2		
Reddish	Category %		11		**44**		12		**35**		19		9		13		**51**		18		21		16		
	# of Events	18		**14**		5		**30**		47		4		7		**38**		164		30		6		363	3
	Feature %		5		4		1		8		13		1		2		10		**45**		8		2		
Bluish	Category %		9		12		12		4		7		11		17		1		20		16		24		
	# of Events	15		4		5		3		17		5		9		1		177		23		9		268	0
	Feature %		6		1		2		1		6		2		3		0		**66**		9		3		
	Feature Totals →	163		32		43		85		249		44		54		75		887		146		37		1815	

Table 6 Cameron, Features vs. Categories

PLATE CAPTIONS

Plate I Distribution of 100 LTP sites on the Moon

A Lick Observatory Composite Photograph of the Moon. Superimposed on it are the 100 features that have been reported more than once as exhibiting Lunar Transient Phenomena (LTP). The twelve features discussed in the text are marked by the **bold** "**X**" symbols while the rest are plusses (**+**). Note the non-randomness of the distribution and the strong affinity to the dark areas (volcanic), and the paucity of sites in the highlands. If the 100 features reported only once were also plotted, their distribution would be very similar.

Image by permission of UCO/Lick Observatory

Plate II Selected Features for Analyses

A montage of lunar photographs courtesy NASA'S National Space Flight Center (NSSDC) cropped from frames of the Lunar Orbiter series of spacecraft, for the 12 features analyzed and discussed in this paper. The spacecraft is designated as LO, followed by the Orbiter number (I, II, III, IV, V) and the frame number in Arabic. There were two cameras aboard each spacecraft, one for medium (M), and one for high magnification in which the section of the frame is given in Arabic numbers, e.g. LO IV 163-3. Each photo is labeled A-P. Some of these photos from the originals were not in the author's possession and were taken from the Gazetteer--NASA SP-241, titled Atlas and Gazetteer of the Near Side of the Moon, prepared by G.L. Gutschewski, D.C. Kinsler, and E. Whitaker.

FIGURE CAPTIONS

Figure 1a Numbers of Observations for Categories vs. Lunar Age

Figure 1b Numbers of Observations for Features vs. Lunar age

Figure 2a Numbers of Observations for Categories vs. Tidal Anomalistic Phase (φ_d)

Figure 2b Numbers of Observations for Features vs. Tidal Anomalistic Period Phase (φ_d)

Figure 3 Plots of Percent for Features vs. Categories

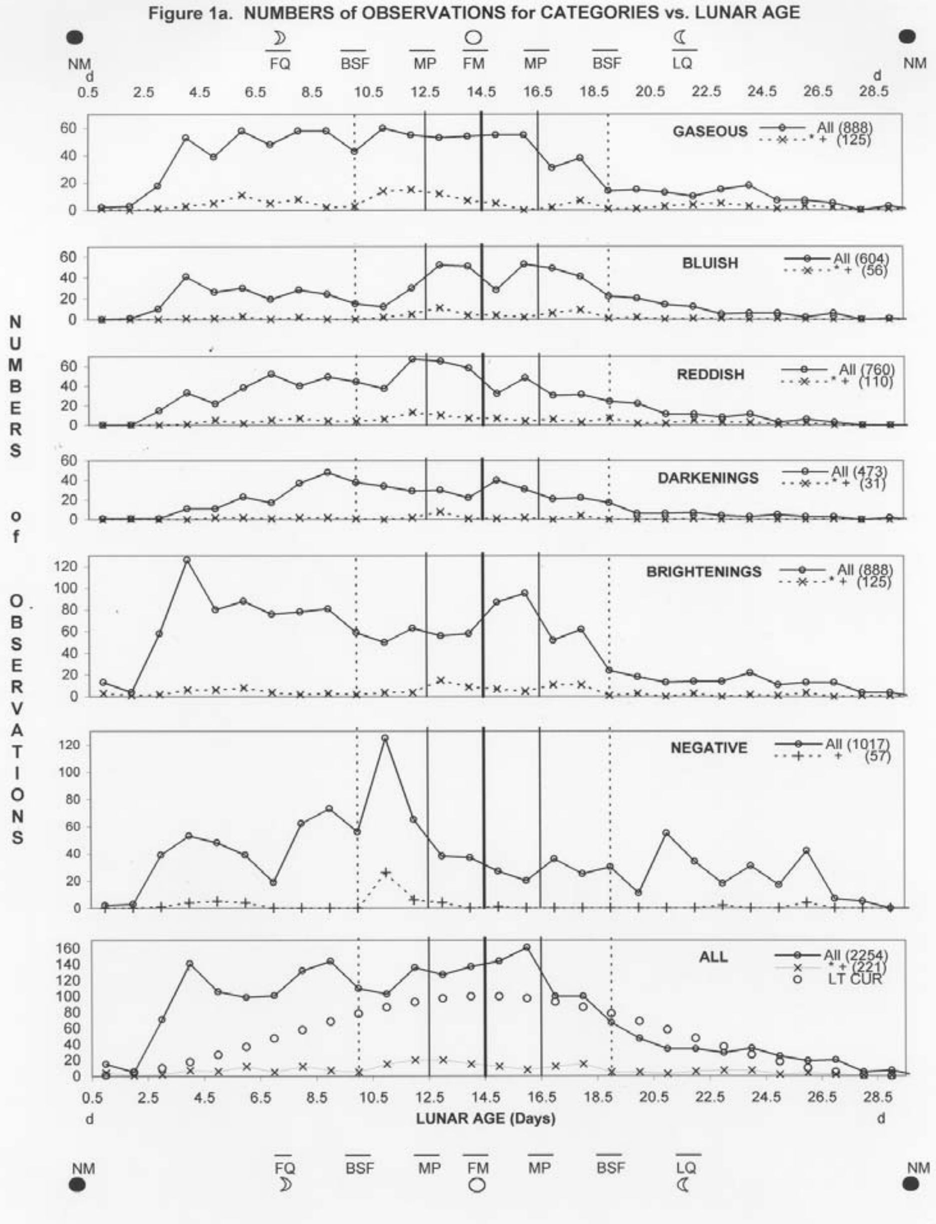

Figure 1a Cameron, Numbers of Observations for Categories vs Lunar Age

Figure 1b. NUMBERS of OBSERVATIONS for FEATURES vs LUNAR AGE

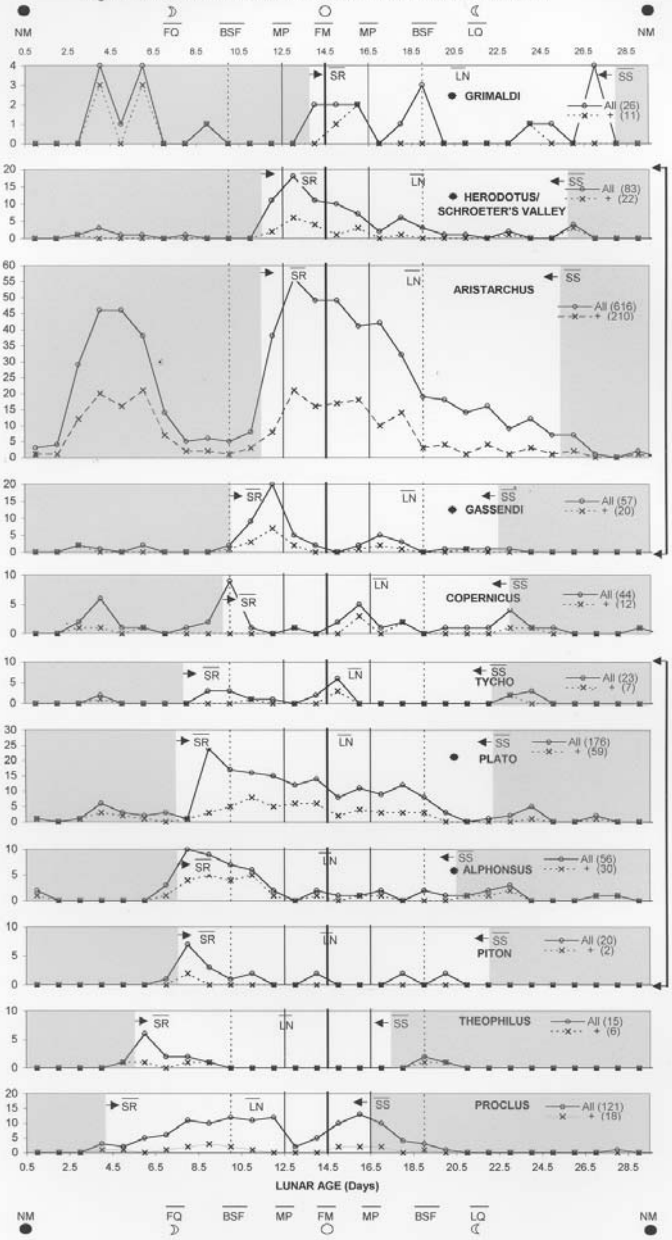

Figure 1b Cameron, Numbers of Observations for Features vs Lunar Age

Figure 2a. NUMBERS of OBSERVATIONS for CATEGORIES vs TIDAL ANOMALISTIC PHASE (φd)

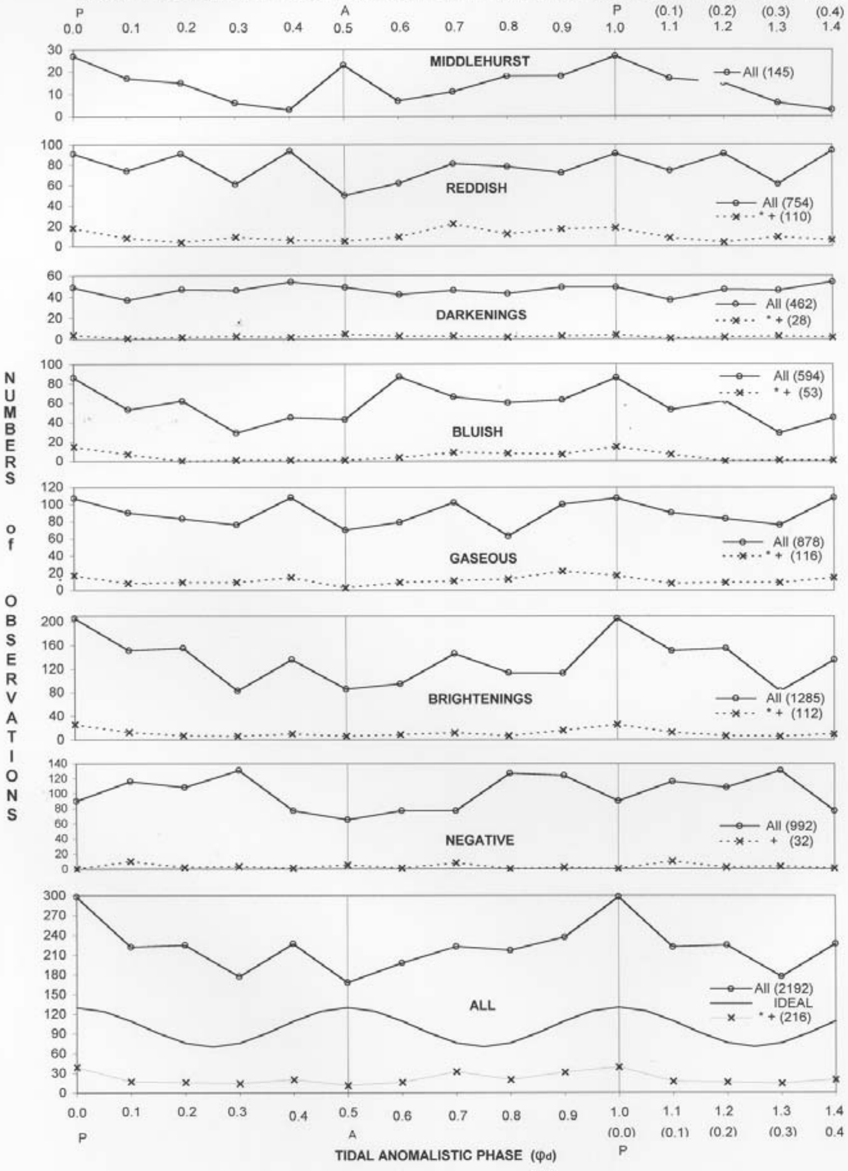

Figure 2a Cameron, Numbers of Observations for Categories vs Tidal Anomalistic Phase

Figure 2b. NUMBERS of OBSERVATIONS for FEATURES vs. TIDAL ANOMALISTIC PHASE (φ_d)

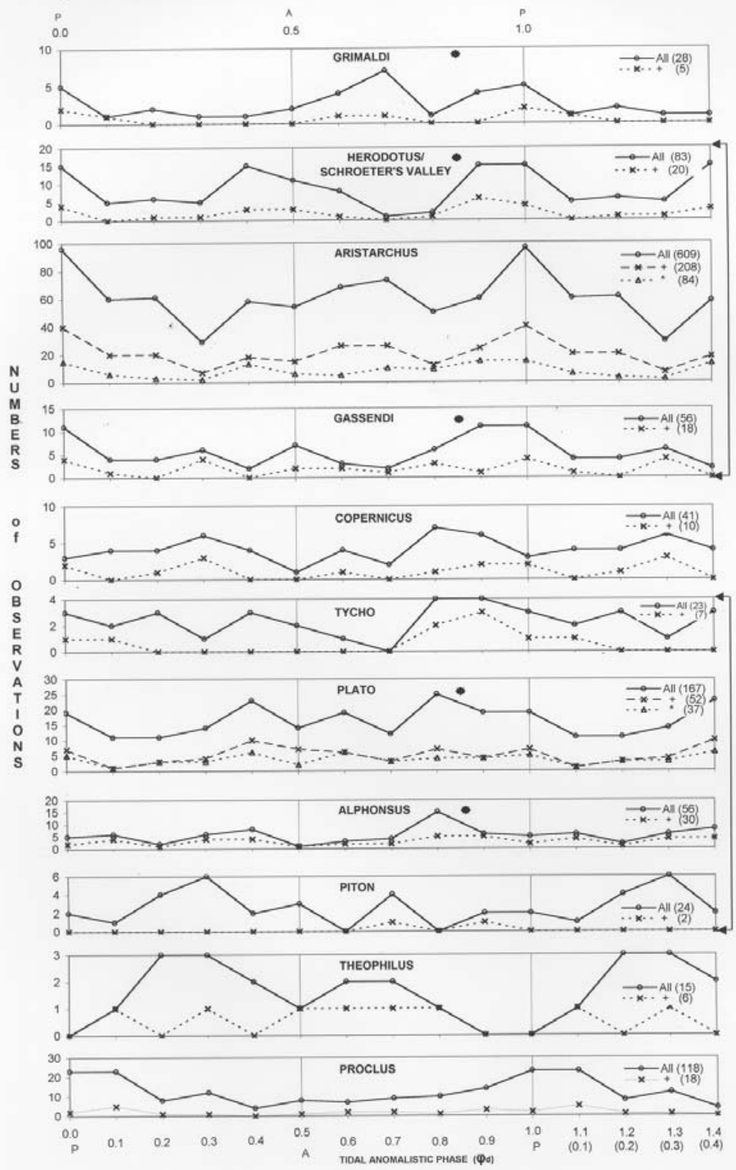

Figure 2b Cameron, Numbers of Observations for Features vs. Tidal Anomalistic Phase (φ_d)

Figure 3 Plots of Percents in Table 6

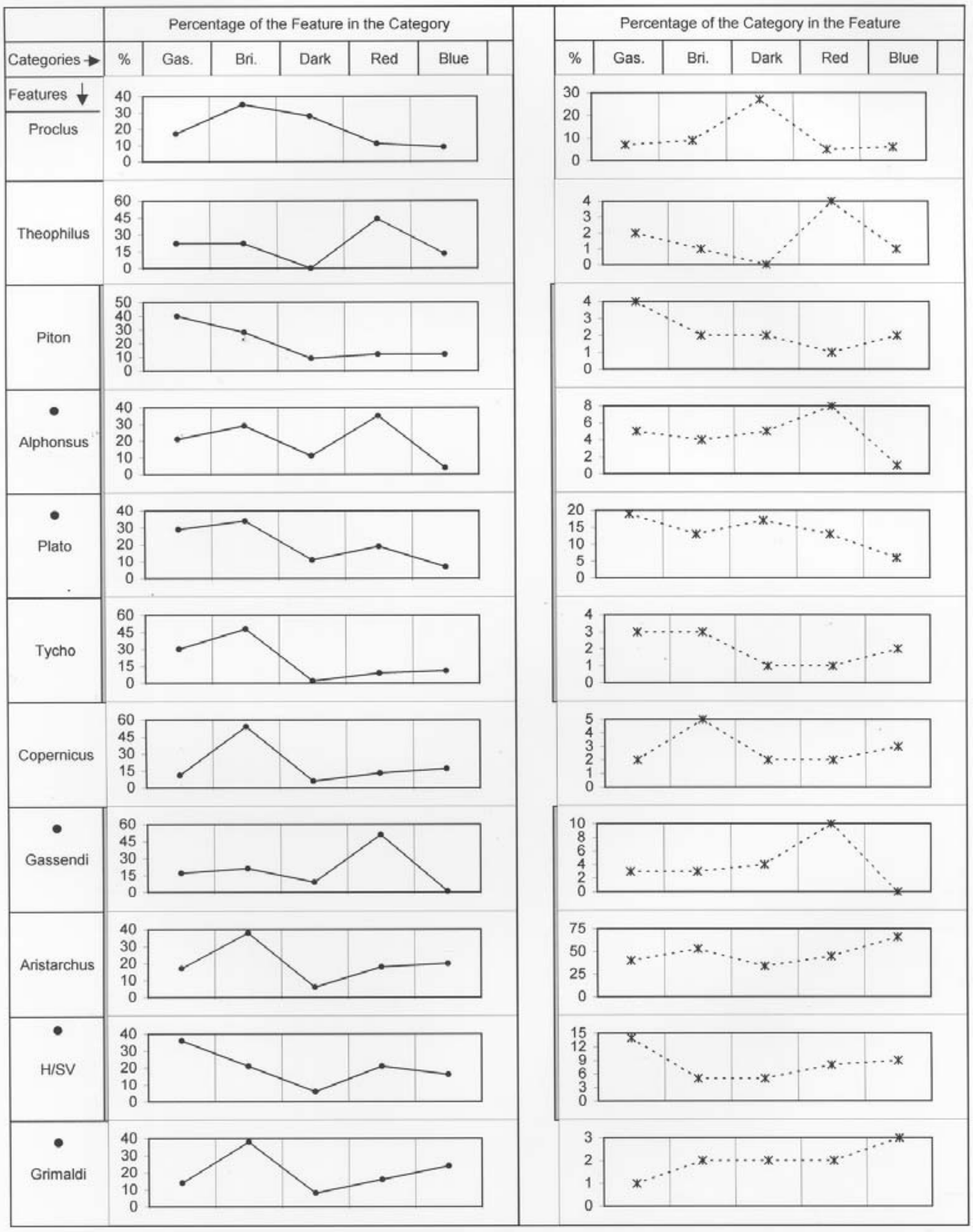

Figure 3. Cameron, Plots of Percents in Table 6